MARLIN JUCHEM

DETAILED INVESTIGATION OF SMALL WATERSHED SYSTEMS IN SOUTHERN PORTUGAL, IMPLEMENTING A MULTI-METHOD RECHARGE ESTIMATION COMPARISON

UNIVERSIDADE DO ALGARVE
FACULDADE DE CIÊNCIAS E TECNOLOGIA
2021

MARLIN JUCHEM

DETAILED INVESTIGATION OF SMALL WATERSHED SYSTEMS IN SOUTHERN PORTUGAL, IMPLEMENTING A MULTI-METHOD RECHARGE ESTIMATION COMPARISON

Master in Marine and Coastal Systems
Work performed under the supervision of:

Dr. Maria da Conceição Lopes Videira Louro Neves
(UAlg, IDL)
Kathleen Elizabeth Standen (UAlg, Faro)

UNIVERSIDADE DO ALGARVE
FACULDADE DE CIÊNCIAS E TECNOLOGIA
2021

Declaração de autoria de trabalho / Declaration of Authorship of work

Declaro ser o(a) autor(a) deste trabalho, que é original e inédito. Autores e trabalhos consultados estão devidamente citados no texto e constam da listagem de referências incluída.

I declare to be the author of this work, which is original and unpublished. Authors and works consulted are duly cited in the text and are included in the list of references.

X

Marlin Juchem

Faro, 28th of September 2021

Copyright

Acknowledgements

Firstly, I would like to thank my thesis supervisors Maria da Conceição Lopes Videira Louro Neves and Kathleen Elizabeth Standen for their support, guidance, advises and especially patience throughout the process of this work. I have gained invaluable knowledge from both of you that I hope to apply in my future. Secondly, I would like to thank the Hydrology department team namely Luis Costa and Kathleen Standen, for including me in their daily research life and sharing their great wisdom of this field. Furthermore, I appreciate the assistance and support you both provided for the fieldwork. And of course, thanks to friends and family, Maren Juchem, Jasmine Haskell, Pedro Rocha and Lala Mills for general moral support that was well needed.

RESUMO

Este estudo aborda uma analise completa da recarga dos aquíferos, assim como os seus factores climáticos e hidrológicos, dentro de um pequeno sistema de bacias hidrográficas em Portugal, na região semiárida do Algarve. Foram coletados na região durante os meses de maior pluviosidade vários diferentes conjuntos de dados derivados, obtidos entre novembro de 2020 e abril de 2021. Dentro das séries de dados há factores como, temperatura, precipitação e evapotranspiração, assim como medidas piezométricas em campo. A distribuição dos factores climáticos foi estudada com o uso de métodos de interpolação de dados em grelha, revelando uma mínima variação espacial na região estudada. O estudo estatístico demonstra uma forte correlação entre os factores climáticos e medidas dos níveis dos aquíferos, sugerindo que há uma resposta rápida dos aquíferos às flutuações climáticas. Os coeficientes de correlação foram 0.7 a 0.8 para precipitação e -0.3 a -0.4 para temperatura e potencial de evapotranspiração. Além disso, foi observado que o próprio sistema do aquífero é bem conectado na região estudada, com coeficientes de correlação maiores que 0.9 para as medidas piezométricas. Ainda, utilizando os dados coletados, múltiplas técnicas foram implementadas na área de estudo para estimar o valor de recarga do aquífero durante o período de observação, resultando em dois modelos de recarga que apresentaram um bom desempenho. Os métodos e as incertezas dos dois modelos, BALSEQ e LUMPREM, foram comparados em detalhes a fim de avaliar a significância e as imprecisões em suas simulações do período de observação. O modelo BALSEQ sugere que a recarga varia de 81.58 a 160.32 mm, e de acordo com o modelo LUMPREM, a recarga varia de 16.97 a 93.67 mm. No entanto, a avaliação do desempenho dos modelos sugere que, nas duas abordagens, a variação dos resultados de sobreposição, entre 80 e 90 mm de recarga, é a mais significativa.

Palavra-Chaves: Água subterrânea; estimativas de recarga; fatores climáticas; hidrogeologia

ABSTRACT

This study includes a thorough examination of groundwater recharge, as well as its hydrogeological and climatic drivers, within a small watershed system in Portugal's semi-arid Algarve region. Several different derived data sets were collected over the region's most significant rain months, over a 5-month period between November 2020 and April 2021. Among the data sets are climate factors including temperature, precipitation, and evapotranspiration, as well as various in field piezometric measurements. Using interpolation methods of gridded data, the geographical distribution of climatic drivers was studied, visualizing and describing the minimal spatial variation within the research region. The statistical study of the climatic factors and measured groundwater levels indicated a strong relationship, suggesting rapid groundwater responses to climate fluctuations, with correlations coefficients of 0.7 to 0.8 regarding the precipitation and -0.3 to -0.4 regarding temperature and potential evapotranspiration. Furthermore, it showed that the groundwater system itself is well connected throughout the region, with most corelation coefficients above 0.9 between the piezometric measurements.

Utilizing the gathered data, multiple techniques to estimate the recharge value during the observation period were implemented on the study location, resulting in two distinct recharge models with good performance. The methods and uncertainties of the two models, BALSEQ and LUMPREM were compared in detail in order to assess the significance and inaccuracies in their simulations of the observation period. According to the BALSEQ model, recharge varies from 81.58 to 160.32 mm, and according to the LUMPREM model, recharge ranges from 16.97 to 93.67 mm. However, the evaluation of performances of the models suggests that the overlapping result range of the two approaches, between 80 and 90 mm of recharge, is the most significant.

Key words: Groundwater; recharge estimation; climate factors; hydrogeology

RESUMO ALARGADO

Numa época de escassez de recursos, a disponibilidade de água representa uma das principais preocupações. De forma a garantir a sustentabilidade dos recursos hídricos é importante que haja uma compreensão adequada do ciclo hídrico (Healy et al., 2007). A água armazenada no subsolo consiste no maior reservatório de água doce disponível ao homem no mundo e contribui para mais de um terço da origem da água utilizada na Terra, sendo por isso um recurso importante para sustentar as necessidades ecológicas e societais no globo (Siebert et al., 2010; Taylor et al., 2013; Wada et al., 2010). Por conseguinte, é crucial examinar e compreender as variações dos níveis das águas subterrâneas e interpretar todos os processos que os influenciam nas condições climáticas atuais e futuras. As crises regionais de falta de água podem resultar da redução dos níveis de água subterrânea, originadas pelo desequilíbrio no ciclo da água, o que é comum em regiões com climas semi-áridos como o Algarve, a província mais a sul de Portugal (2019; Miranda et al., 2002; Soares et al., 2017).

Este estudo centra-se numa pequena bacia hidrográfica localizada no Algarve e visa analisar aprofundadamente todos os processos que interagem com o ciclo da água local, de forma a estimar as volumes de recarga. O sistema de águas subterrâneas da região é dominado por quatro aquíferos interligados: o subsistema de Vale de Lobo (M18), o subsistema de Faro (M19), o São João da Venda-Quelfes (M10) e o Almansil-Medronhal (M9). A variação dos níveis de água subterrânea dentro e entre estes sistemas é controlada pela geologia e topografia local, proximidade ao oceano e as forças motrizes associadas o clima semi-árido. As formações geológicas que sustentam estes aquíferos são compostas principalmente por camadas sedimentares do Jurássico, Cretáceo, Mioceno, Holoceno e Plio-Quaternário. A inclinação a sul destas formações, combinado com a tectónica regional, bem como as características semi-cársicas de algumas das formações, fazem desta região um ambiente muito heterogéneo com condições hidrogeológicas muito variáveis na área de estudo. (Neves et al., 2019; Stigter et al., 1998).

O clima da região é tipicamente mediterrânico. Um dos principais problemas associados à gestão de água na região reside na irregularidade do regime de precipitação, que apresenta longos períodos de seca nos meses de verão e períodos intermitentes de chuva forte nos meses de inverno. A média mensal de temperatura varia entre 11 e 26.5 °C com uma precipitação anual total de cerca de 620 mm/ano. Aproximadamente 50% da precipitação anual ocorre nos três meses de dezembro e Fevereiro (Miranda et al., Nunes et al., 2006).

De forma a alcançar os objectivos propostos neste estudo, nomeadamente, avaliar e estimar a recarga directa da precipitação durante o período ocorrido entre 18.11.2020 e 12.04.2021, foram recolhidos, analisados e processados vários conjuntos de dados, que, após o pré-processamento foram utilizados como dados de entrada de diferentes modelos de recarga. A recolha de dados inclui séries temporais piezométricas de 5 locais diferentes que foram recolhidos utilizando ctd-datalogger, seguindo uma orientação de Sul (junto a costa) para Norte (no interior Algarvio), originando 5 conjuntos de dados de nível das águas subterrâneas durante o período observado.

Os dados climáticos foram recolhidos a partir da estação meteorológica da DRAP Algarve, localizada no Patacão, Faro (DRAP, 2021), por ser a mais próxima dos pontos de observação piezométrica. Para investigar a variabilidade espacial dos dados climáticos, analisaram-se as grelhas de dados disponibilizados pela ECMRWF - *European Centre for Medium-Range Weather Forecasts* (ECMWF, 2012) descarregados e transformados de acordo com a região. As principais variáveis climáticas consideradas para este estudo foram a temperatura do ar [°C], a precipitação [mm] e a evapotranspiração potencial [mm], todas medidas com frequência diária.

Os diferentes conjuntos de dados foram pré-processados, com métodos de remoção de tendência e normalização, de forma a permitir a sua comparação. Numa análise inicial, os dados pré-processados foram submetidos a uma análise estatística, que incluiu o teste de correlação entre cada conjunto de dados e a correlação cruzada entre os níveis piezométricos e as forças climáticas. Os resultados desta análise sugerem uma alta correlação entre as variáveis climáticas, especialmente a precipitação com os níveis de água subterrânea (com coeficientes acima de 0,7), além disso, a correlação cruzada não apresentou um desfasamento entre os fatores climáticos e os níveis piezométricos, indicando uma resposta imediata às variáveis climáticas.

Com base nas características estatísticas calculadas, procedeu-se à estimativa de recarga com recurso aos modelos seleccionados.

De acordo com os dados disponíveis, o clima regional e os atributos hidrogeológicos da área de estudo, foram escolhidos dois modelos distintos para serem aplicados no âmbito deste estudo, o modelo BALSEQ e o modelo LUMPREM. Embora ambos os modelos sejam modelos de parâmetros agrupados, com base na abordagem do equilíbrio da humidade do solo, estes diferem fortemente na sua complexidade e resultados. O modelo BALSEQ (Ferreira, 1981; Ferreira & Rodrigues, 1988) assemelha-se a um modelo conceptual simples, que usa dados de precipitação e evapotranspiração potencial como dados de entrada e que pode ser calibrado de acordo com pressupostos de estudos anteriores (Ferreira & Rodrigues, 1988; Martins et al., 2021). As estimativas de recarga obtidas com o modelo BALSEQ para o período em estudo variaram entre 81.58 e 160.32 mm.

O modelo LUMPREM (Doherty, 2020), mais complexo, foi calibrado especificamente para cada ponto de observação piezométrica, ajustando manualmente os parâmetros de calibração para alcançar a maior correlação entre os valores observados e simulados. Apesar de utilizar os dados climáticos de entrada, este modelo sugere valores de recarga mais reduzidos em comparação com a abordagem BALSEQ, variando entre 16.97 e 93.67 mm.

No que diz respeito às diferenças de ambas as simulações, os dois modelos foram comparados de acordo com o seu desempenho na área de estudo, concluindo que ambos têm as suas vantagens e desvantagens e complexidade. Isto sublinha a importância de uma análise com múltiplos métodos, de forma a minimizar a imprecisão associada ao uso de um único modelo, uma vez que a gama de valores de recarga sugerida por ambos os modelos pode ser a mais significativa. Além disso, este trabalho demonstra a importância para a continuidade de trabalhos de investigação neste domínio, uma vez que uma gestão eficiente de um recurso tão importante como a água só pode ser feita de forma eficaz, quando estes valores de recarga são conhecidos.

Table of Contents

LIST OF FIGURES

LIST OF TABLES

LIST OF FUNCTIONS

1 INTRODUCTION

In an era of resource scarcity, the availability of water is an important concern. Ensuring the sustainability of water supplies demands an adequate understanding of the water cycle (Healy et al., 2007). Freshwater is an essential resource for humans and ecosystems. With more than one third of the used water originating from beneath Earth's surface, groundwater systems are the world's largest distributed store of freshwater and therefore critical for sustaining global ecological and societal needs (Siebert et al., 2010; Taylor et al., 2013; Wada et al., 2010). In most environments, natural groundwater function as buffers against climate extremes, sustaining the baseflow to rivers, lakes and wetlands in periods of low or no precipitation. Global resources of freshwater are under increasing threats, due to the contemporary evolution of the climate (le Houérou, 1996). With increasing temperatures and shifts in the meteorological processes, climate change exacerbates regional drought events and desertification (Helldén & Tottrup, 2008). Land degradation (Besser et al., 2017), frequent wildfires (Gouveia et al., 2012; Jolly et al., 2015) and regional water crises can be results of the depleted groundwaters, initiated by the imbalance within the water cycle (Famiglietti, 2014). This particularly affects regions with semi-arid climates like the Algarve, the most southern province of Portugal. Future rainfall predictions for Portugal, particularly in the southern region, are indicating a decrease in precipitation and a temperature rise (Cardoso et al., 2019; Miranda et al., 2002; Soares et al., 2017). With the rapid increase of the population, expanding aeras of irrigated agriculture and the higher probabilities of severe drought occurrences (Marvel et al., 2019; Spinoni et al., 2018), groundwater systems are dramatically affected by anthropogenic pressures together with climate change.

Consequently, it is crucial to examine and understand how groundwater levels (GWL) change and respond to all processes influencing them under present and future climate conditions. It is especially important to study the influence of climate factors on the volume of water that comprises the recharge (Scibek & Allen, 2006), as this is a crucial element in the equation of water balance and an essential parameter for the efficient management of water resources (Maréchal et al., 2006). For the development of a sustainable usage of groundwater systems, the sources exploitation should never exceed the recharge rate of its correspondent

groundwater basin (Moon et al., 2004). The Water Framework Directive established by the European Commission (European Commission, 2015), defines the quantitative status of a groundwater system by the usage of the annual water quantity compared to the long-term annual recharge. Furthermore, the Framework Directive states that only when the yearly abstraction rate is less than 90% of the overall average recharge rate, an aquifer system may be classified with a good quantitative status. While these requirements play an important role for groundwater management, to justify and enable these types of classifications as well as to define the state of a single system, values of high significances must be established and presented. Once again this emphasizes the need of accurate recharge models and investigations.

This study focuses on the groundwater fluctuations within the aquifers of the Ria Formosa lagoon in Faro, Portugal, a wildlife reserve of high importance for the regional ecology and economy. A good understanding of the natural fluctuations related to climate forcing is the base for further evaluations, improved modelling and effective management in this region (Neves et al., 2019).

1.1 Objectives

The aim of this study is to evaluate and model the groundwater recharge of a semi-karstic, small watershed system over a 6-months winter period in the semi-arid climate of southern Portugal. Within the scope of this work, climate drivers are related to piezometric groundwater measurements, and their interdependencies are implemented into several numerical groundwater models to better understand the key variables of the local recharge events.

An estimation of the groundwater recharge must include all forces and characteristics that determine the water fluctuation within the observed region. This includes not only meteorological aspects such as precipitation and temperature regarding their time scales and frequencies, but also physiographic characteristics of the region determined by regional geology and morphology of ground and soil, large-scale structures like faults and the vegetation or other land uses and covers (Cambraia Neto & Rodrigues, 2020). As all these factors can strongly vary from one location to another inside a catchment area, this project

will include a collection and analysis of several measurements spatially distributed over the study region. The range and coverage of measurements enable a good interpretation and understanding of the fluctuations and recharge processes of the regional groundwater system and how they spatially vary.

Hydrological models are typically used to gather insights of groundwater systems and their connection to the water cycle to generate recharge predictions and evaluate the sustainability of the water use of a region (Meixner et al., 2016). However, given the site-specific forcing factors for water fluctuations, it is important to select the most suitable recharge model to generate a relevant recharge prediction (Moeck et al., 2018). As different methods of modelling and predicting use a variety of structures and parametrizations, their selection can strongly affect the quality of the results (Breuer et al., 2009). In this work, the collected data will be considered as input for several models and approaches of recharge estimation. The most suitable method is to be selected depending on the final quality of the collected data and the functions and variables available within each method, the most suitable method for this study area will be used to compute an estimation of recharge.

1.2 Groundwater Fluctuations & Recharge Processes

The quantity of water within a groundwater system is commonly represented as fluctuations in the GWL. These fluctuations within groundwater systems are governed by a dynamic reciprocity between recharge and discharge. Several forcing factors and a variety of responses including climate, soils, vegetation or other land covers and human abstraction highly influence these dynamics. These variations can be of different time scales, magnitude and follow different patterns according to the drivers. In regard to the hydrological cycle, climate is the major force, as it controls precipitation, atmospheric pressure and temperature at various spatio-temporal scales (Orlanski, 1975). All these variables are strongly connected to the amounts of soil infiltration, deeper percolation and evapotranspiration, which finally determine the groundwater recharge (Wu et al., 2020). In addition to these surface derived influences, the boundary condition between two aquifer systems, depending on their linkages, may lead to interactions with effects of similar amplitude. (Cuthbert et al., 2019).

Recharge is defined as an addition of water to an aquifer or groundwater system from the overlaying unsaturated zone or a surface water body and can be divided into diffuse (direct) recharge and focussed (indirect) recharge. While diffuse recharge explains the process including water originating from precipitation or irrigation over large areas, the focused or localized recharge refers to streams and lakes or other topographic depressions e.g., faults and sinkholes. Processes as infiltration, drainage, percolation and seepage control the water movement from the surface to the subsurface, below the root zone and to deeper aquifer systems, however their relationships are highly non-linear and usually cannot be measured directly. The discharge, movement of groundwater through the subsurface or the surface, can occur naturally via springs, streams, lakes or wetlands and in response to anthropogenic activity by groundwater abstraction. Subsurface water can also directly discharge back to the atmosphere by the uptake of water by vegetation through the root zone. The process of evapotranspiration particularly plays a major role in regions of arid climates, which have a strong excess of evapotranspiration over the precipitation, leading to large unsaturated zone thicknesses and ephemeral streams that may disconnect the underlaying groundwater system, and therefore have no baseflow.

The aforementioned processes, inducing the movement of subsurface waters, are strictly connected to the regional geological composition, lithology, morphology and topography. Various types of solid rocks, mineral grains and organic matter contribute to the earth's subsurface. The composition of a geological medium is given by the percentages of the different components it is made of, these can vary in grain size, shape and in their molecular structure (Healy et al., 2007; Morris & Johnson, 1967). The attributes of the geological medium determine the hydrological properties such as porosity and permeability. Porosity describes the ratio between pore space or voids and total volume of the medium. Primary porosity refers to the space within granular material (e.g., sedimentary rocks with pebbles and grains) and secondary porosity is related to fractures (e.g. joints and faults) in consolidated rock. The porosity of a medium positively correlates to its permeability. Permeability or hydrological conductivity is the measure of the material's ability to transmit water (Lohman, 1972).

The geological composition within an area can vary vertically in terms of lithological strata, geological layers of different eras including structures and formations created by the

dominant processes of each time period, and horizontally due to changes in morphology and topography. The vadose zone plays a pivotal role in the link between hydroclimatic forcing and groundwater recharge. The vadose zone or unsaturated zone is the geological structure between the land surface and groundwater table of the upper unconfined aquifer (Arora et al., 2019). All physical processes within this zone determine the transmission of water between the atmosphere and aquifers.

All hydrodynamic processes and the balance between them determine the total recharge of a groundwater system (Aguilera & Murillo, 2009; Allocca et al., 2015; Jourde et al., 2015). For higher investigative methods or models to compute or predict recharge values, it is mandatory to understand the general flowing concepts of water in porous medium and the interplay between hydrological conductivity, climate induced temperature and gravity given for each region (Mazzilli et al., 2019).

1.3 Recharge Estimation Methods

Whilst the mathematics behind all the physical processes and factors (e.g. surface runoff, infiltration, percolation, crop and surface vegetation) are well known and can be simulated within numerical models, they typically have extensive data requirements of parameters which cannot be measured in the field, especially at the scales of aquifer systems. Even when measured in laboratorial conditions that try to replicate the study site's attributes, the resulting parameters are unlikely to be applicable or relevant for a simulation that attempts to connect all the processes within a whole aquifer.

Several approaches including different methods or models to estimate and compute regional and global recharge rates have been established in the past (Aguilera & Murillo, 2009). Each approach has its own limitations regarding factors as applicability and reliability, and particular techniques need to be chosen under consideration of hydroclimatic characteristics of the observed area, the available data and financial and technical resources (Aguilera & Murillo, 2009; Moeck et al., 2018).

Automated groundwater hydrograph analysis techniques that have been developed in the past, are usually based on digital filters and recession curve analysis (Arnold & Allen, 1999; Rouhani & Malekian, 2013). Other methods based on water-balance equations (Lewis &

Walker, 2002) or general-purpose numerical models based on soil-plant-atmosphere systems (Crosbie et al., 2012) have been developed for various regions. Mathematical based models use simple analytical functions that approximate the basic behaviour of a system, with additional inputs of empirical and theoretical variables (Nimmo & Perkins, 2018). The complexity of these functions can strongly vary, depending on the number of variables, time scale and measurements included within the calculation. However, including more variables does not necessarily increase the accuracy of a model, since this will also result in an increase of uncertainties and errors (Aguilera & Murillo, 2009). Amongst all these developed estimation methods, the most commonly used are the Chloride Mass Balance, the Water Table Fluctuation method, Environmental Tracer method, Soil Moisture Balance method and Groundwater Recovery and Climate Experiment (Table 1), or further developed or adjusted variations of these according to the area they are applied to. These diversities of models have covered regions with similar climate and/or similar geological properties as found in the Algarve (e.g., Aguilera & Murillo, 2009; Allocca et al., 2015; Mazzilli et al., 2019), confirming decreasing recharge values and therefore a loss of available groundwater resources due to climate change, and indicate the need for further research in this field for a better evaluation and understanding of the usage of the variables included in the models.

As this study attempts to estimate the recharge within the small water sheds of the Algarve, a system that is highly determined by the intense use of the surrounding agriculture and interacts with water derived from the sea due to its proximity to the Atlantic Ocean, the possibilities of applicable model baselines presented within Table 1 are reduced to approaches that follow the baseline of the Soil Moisture Balance method.

While the recharge processes including an estimate of recharge have been investigated within the work of Ferreira & Rodrigues (1988), it remains unclear in what scale the spatial differences in this region affect these estimations, furthermore how the system is controlled by the “modern” climate. Other more recent approaches of applying soil balance base models within the Algarve by Hugman et al., (2012) and Salvador et al., (2012) with higher spatial distributed results indicate that especially towards the south, estimations tend to vary strongly and depict the difficulties that come with the efficient quantification of these systems.

Table 1: List of most common used recharge estimation methods, including a general description of each models' approach, as well as their advantages and disadvantages.

Methods	Description
Chloride Mass Balance	This approach is set up under the assumption that chloride has a conservative behaviour within the water cycle, i.e., it remains when introduced to a groundwater system. Cl contained in the rainfall and the rainfall volumes is measured, the measured amount of Cl within the groundwater can then be used to estimate the recharge after the runoff has been well simulated (Aishlin & Mcnamara, 2011). Advantages: This approach is very cost efficient and easy to apply. Disadvantages: This method cannot be used within systems that are connected to seawater or located in geology originating or formed within oceanic or coastal environments, as these systems by default include high amounts of Cl.
Water Table Fluctuation Method	This method is commonly used. It measures GWL rises in relation to rainfall and calculates the recharge by estimating a specific yield within the system, which is mainly determined by the hydrological conductivities and size of the aquifer (Liang & Zhang, 2012). Advantages: This approach is usually very easy to apply within its simplicity. Disadvantages: The approache's principal is not applicable when the groundwater fluctuations are covered or altered by other signals such as irrigation. The needed specific yield is very hard to estimate and to justify for entire aquifers. The method's accuracy can only be justified when there is available data of discharge and abstraction.
Environmental Trace / Isotope Tracing	This method uses anthropogenic gases such as Chlorofluorocarbon (CFC) or Sulfur hexafluoride (SF6) and stable isotope and their decay such as C14, Cl 36 and Tritium. These tracers are used to show the presence of modern water and its residence time within a water body (Turnadge & Smerdon, 2014). Advantages: Usually applicable in any system it gives great insights of the processes and flows within the system. Disadvantages: This method does not result in recharge quantifications or only in rough estimates under very vast assumptions of the system. Due to its sensibility, it only shows significant result when several traces are investigated, which makes its application expensive.
Soil Moisture Balance	This approach is often used as the baseline for models of higher complexity. Diffused recharge estimations are conducted by balancing the water stores on the soil on monthly or daily time steps. When the balance suggests an overwhelmed soil moisture storage, the excess of water is divided into runoff and recharge (Sitch et al., 2003). Advantages: In the past, this type of modelling has been excessively used, leading to well-developed calibrations and additional factors to increase its significance. Disadvantages: For good results this model type needs to be calibrated with variables which are usually hard to assess, especially in heterogeneous systems.
Grace (Groundwater Recovery and Climate Experiment)	In this method, two satellites are used to measure the geoid, the recorded gravity variations are then re-computed to estimate the fluctuations within water bodies (Tapley et al., 2004). Advantages: This method gives accurate monthly changes within water systems. Disadvantages: Due to its remote origin, this approach has a very low resolution of 400 x 400 km and needs a lot of additional modelling and corrections to be accurate.

2 STUDY AREA

2.1 Location and Geology

The observed region is located north of the city of Faro and south of the Caldeirão mountain range, which forms a natural barrier to atmospheric circulation. The groundwater system in the region is dominated by three aquifers (Figure 1): The Campina de Faro (M12), the São João da Venda-Quelfes (M10) and Almansil-Medronhal (M9). Due to its size and differences in water quality and quantities within its system, the Campina de Faro aquifer was recently reclassed into two subsystems by the Portuguese Environment Agency (APA, 2021): The Vale de Lobo subsystem (M18) and the Faro subsystem (M19). The area's relief decreases from north to south with the northern parts of M9 and M10 being close to the slopes and exposed to southerly fluxes from the sea, whereas the relief in the southern parts, namely Campina de Faro M12, is relatively flat (Neves et al., 2019; Stigter et al., 1998). The lithological layers and their hydrological attributes have been described in several studies (Hugman et al., 2017; Neves et al., 2019) and have shown to strongly influence the shape and boundaries of the three aquifers (Figure 2). Due to the general dip to the south, the northern part of the region is characterized by older formations of the Mesozoic and the southern part by younger formations of the Tertiary (Stigter et al., 1998). System M9 is mainly composed of a south dipping (20 - 40°) dolomite and limestone formation from the Upper Jurassic era and can be classified as a karst aquifer (Figure 3). System M10 is composed of a thick sequence of marly limestone and overlying fine detrital sediments (silt and sand), both from the Cretaceous. While the younger units from the Cretaceous (upper part of the unit) interbed with the oldest layers of the Miocene and are most likely to form an aquifer within the M12 boundaries. The older formations of the Cretaceous (lower part of the unit) are predominantly formed of a clayey composition, which acts as an aquitard (confining layer) separating the M10 aquifer from M12 (Francés et al., 2014, 2015). System M12 is a multi-layered unit comprised of three different formations from different eras (Stigter et al., 1998, 2006). The deepest formation is mainly formed by limestone with interbedded marl layers from the Cretaceous. The overlying sub-aquifer system is composed of a formation of sandy limestone from the Miocene deposited in graben-like structure, which bounds in a large N - S trending fault. These Miocene formations can exceed a thickness of 200m.

The Upper layer of this system mainly contains plio-quaternary weathered red clays with sands and gravels in the younger formations. There is evidence of silt and clay depositions from the Holocene (Figure 3). These layers of fine sediments between the Miocene and Plio-Quaternary units with possible lateral discontinuity have an average thickness of approx. 10 m and could have confining effects on the system.

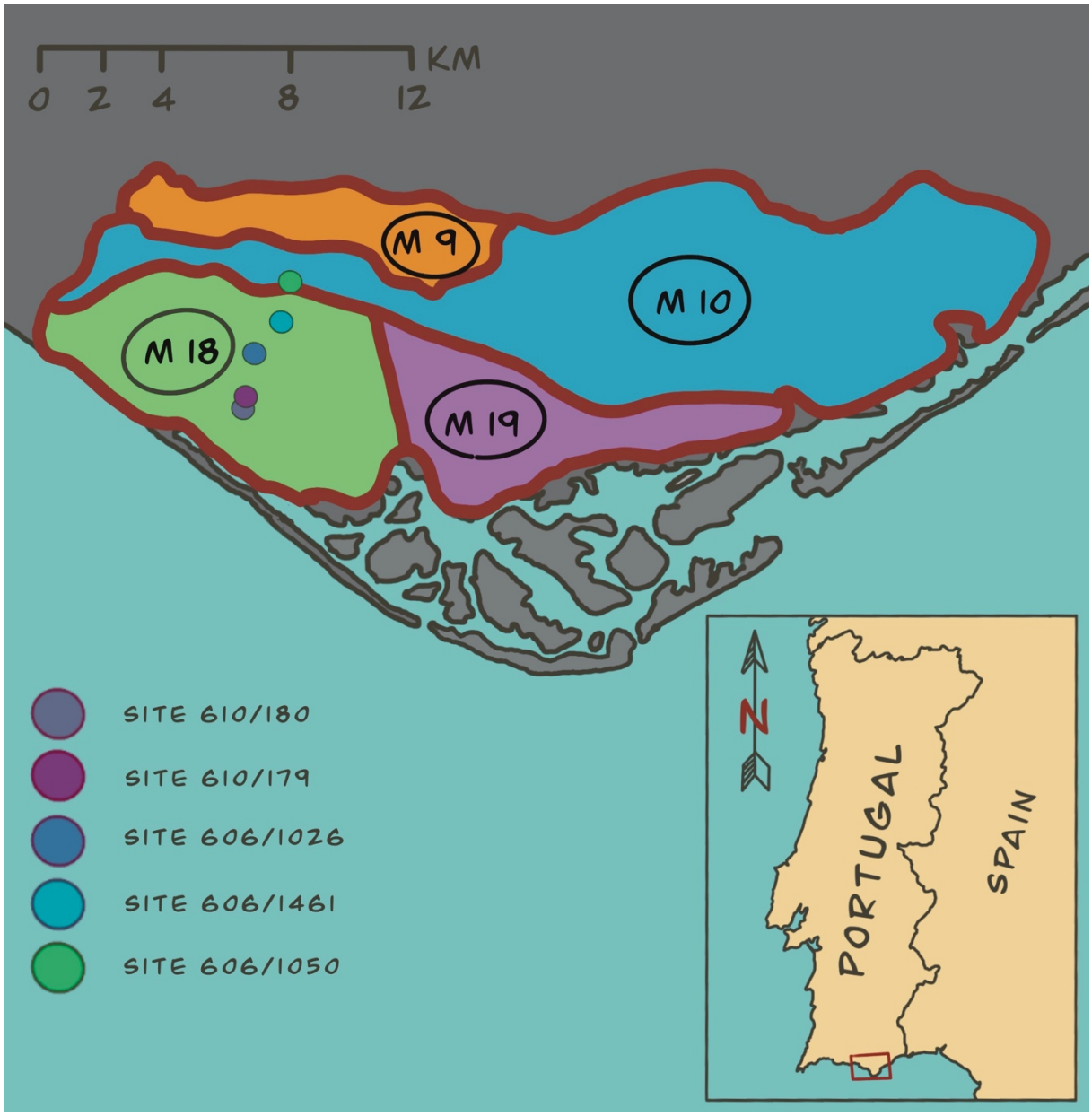

Figure 1: Map of study area showing the boundaries of the different aquifer systems and the locations of the sampling sites.

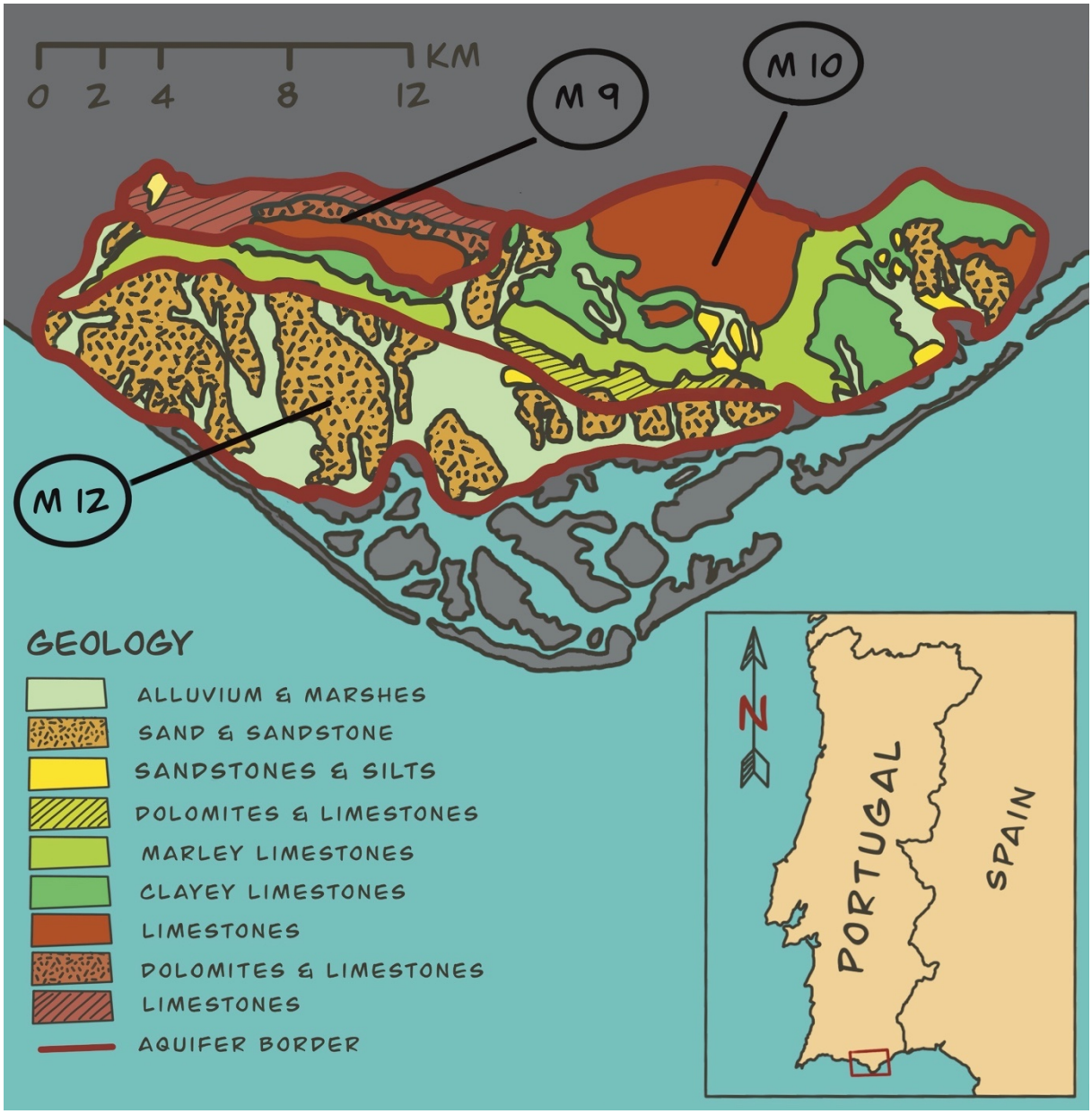

Figure 2: Geological map of the study area, showing the outcropping geology within each aquifer system.

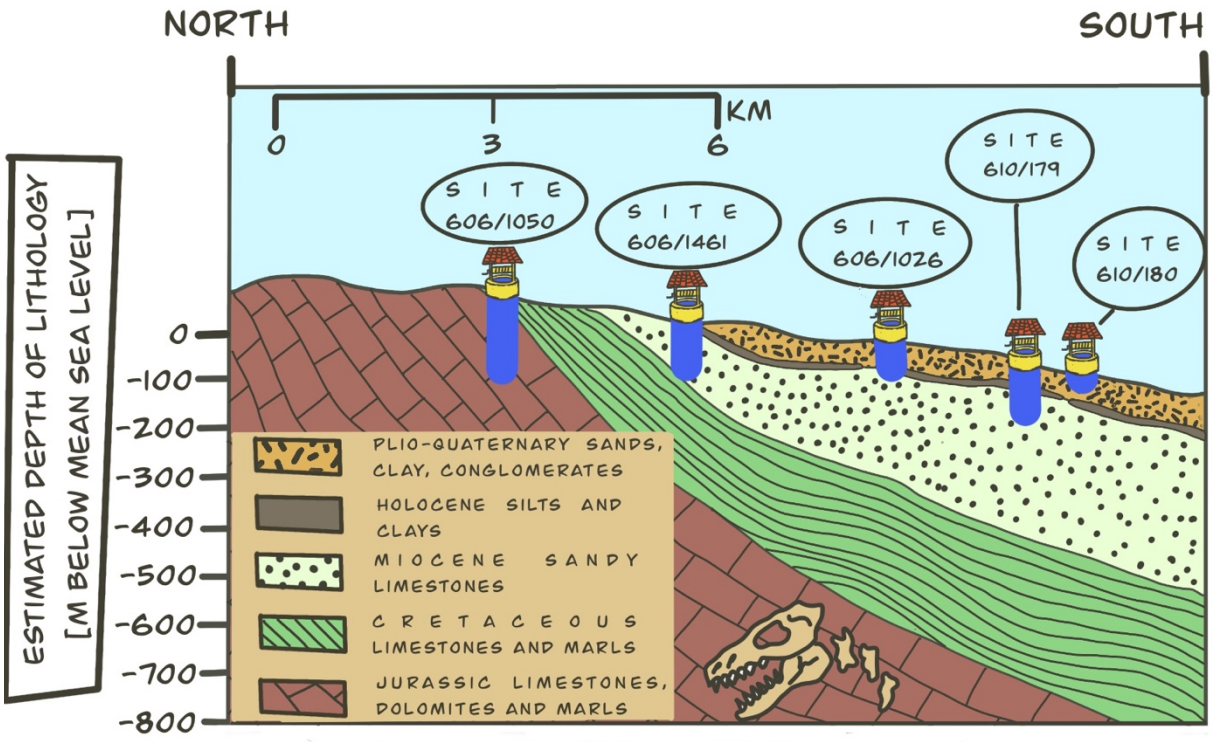

Figure 3: Conceptual cross section of the study area, showing the different lithologies and their relative thickness, as well as the location of each measuring site and the depth/ lithology they operate in (blue marking underneath sites).

2.2 Regional Climate

The climate in the Algarve region in southern Portugal (SW Iberia) is typically described as Mediterranean, classified as type Csa in the Köppen-Geiger (Kottek et al., 2006). Portugal's climate is primarily determined by its location between the sub-tropical anticyclone and the subpolar depression zone. Smaller scaled spatial variability within this zone is affected by latitude, orography and the Atlantic Ocean. The abundance of these spatial variability inducing factors and their effect on the local climate are clearly observable in the Algarve. This leads to significant variances especially regarding the air temperature and primarily the precipitation (Miranda et al., 2002; Neves et al., 2019). One of the major problems of this region lies in the irregularity of the precipitation regime, having long dry periods in the summer months and intermittent periods of strong rainfall in the winter months. Occasionally, this pattern can be intensified by extreme events such as interannual periods of droughts (Nunes et al., 2006). The monthly temperature average is between 11 and 26.5 °C with a total annual rainfall of about 620 mm/year (IPMA, 2021; SNIRH, 2021).

Approximately 50% (Miranda et al., 2002) of the annual precipitation occurs within the three-month window between December and February. This strong cyclic distribution of the rainfall events in the winter seasons determine the available amount of water for the following months.

3 METHODS

3.1 Data Collection

3.1.1 Piezometric Measurements

The piezometric measurements were collected between 18. November 2020 and 12. April 2021 with Van Essen CTD-Datalogger (van Essen, 2021) in 5 different locations within the M12 Aquifer following a line from the coast to the inland, from South to North (Figure 1 & Table 2). The different measuring sites use boreholes that intersect with the geological strata, depending on their depth and location (Figure 3). While the sites 610/180 and 610/179 are less than 10 m apart, their boreholes reach different depths. Site 610/180 uses a borehole with a depth of around 45 m, measures within the unconfined shallow aquifer system in the Plio-Quaternary. The borehole site 610/179 is around 120 m deep, meaning it intersects with the Miocene. Sites 606/1026 and 606/1461 both intersect with the lithology of the Miocene. Due to its northern location, Site 606/1050 is likely to intersect with the lithology of the Jurassic, whilst using a borehole of around 100 m depth.

The dataloggers were programmed to sample with a 15-minute time interval. Before and after each installation the ground water level of each site was manually sampled to confirm start and end values of the time series, with a second source, using a manual water level meter (dip meter).

The initial dataset derived from the CTD's were firstly adjusted to the barometric pressure, this step is crucial as water levels in boreholes are highly affected by atmospheric pressure. This barometric pressure correction was obtained within the Van Essen calibration and download software (Diver Office, van Essen, 2021) which corrects the measured groundwater levels according to the measurement of an CTD-Datalogger that was calibrated to only record barometric fluctuations. Furthermore, the time series were manually cleaned from human induced outliers, that may have occurred during the installation time or by further contacts or impulses during the sampling period. Prior to further use of the measurements, each data set unit was transformed from mm to m and from depth to groundwater head to piezometric level in relation to the mean sea level, by using the ground elevation of each site (SNIRH, 2021).

Table 2: List of sites, the aquifers they are located in and their coordinates

Site	Aquifer	Latitude	Longitude
610/180	M12 – Campina de Faro	-8.00803	37,04425
610/179	M12 – Campina de Faro	-8.00804	37,04427
606/1026	M12 – Campina de Faro	-8.00527	37.06324
606/1461	M12 – Campina de Faro	-7.99577	37.07302
606/1050	M10 - São João da Venda-Quelfes	-7.99307	37.08195

3.1.2 Climate Data

The various climate variables were collected from data bases provided by the DRAP Algarve (Direcção Regional De Agricultura E Pescas Do Algarve) and the ECMRWF - European Centre for Medium-Range Weather Forecasts (DRAP, 2021; ECMWF, 2012) The data set provided by DRAP Algarve are directly measured from a weather station located in Patacão, Faro (37° 02' 48,8'' N; 07° 56' 49,8''W) and provides daily measurements of air temperature (°C 1.5m above ground), total precipitation (mm) and potential evapotranspiration (mm), which is calculated from the weather data by the method of Penman-Monteith (Howell & Evett, 2001). The ERA5 reanalysis data from ECMRWF provides spatial distributed estimates with a native resolution of 0.1° x 0.1° (9km), including the variables air temperature (K 2m above ground) and total precipitation (m).

The minor gaps of both data sets were filled with linear interpolation. In order to evaluate the differences between climate data sets of different origin and the reliability of the records, the Pataçao weather station records and the ERA5 reanalysis computations were compared.

To compare the reanalysis data to the more accurate weather station measurements, the ERA5 grid was transformed into a single time series including the average precipitation and temperature over a square between 37°0’N; -8°2’E and 37°4’; -7°6’N. To visualize the spatial distribution of the climate factors and their variability between the summer and the winter season, the grid data was subsampled and averaged over the winter period/period of field observations (18. November 2020–12. April 2021) and the previous 6 months (1. June 2020 –

1. September 2020). This spatial distribution of the precipitation during the seasons was transformed into contour lines over a geographic map with the use of nearest-neighbour interpolation. A more detailed investigation of the spatial differences of the climate variables between the study sites, was conducted by isolating the exact pixels that cover the study area and using trilinear interpolation methods. Four single time series that show the differences between the climate variables over the observation time could be extracted and compared, with the resolutions that is provided by that ERA5.

3.2 Processing & Statistical Analysis

In order to compare the multiple variables and detect their effects on each other with linear regression and correlations tests, the raw data had to be pre-processed to ensure statistical relevant results. For the pre-processing, the raw data sets were manipulated with Python scripts. The scripts were written to resample, interpolate, detect and remove outliers and export the variables into single files. To compute correlations between the processes recorded with different sampling intervals, the data was resampled to daily intervals by calculating a daily mean value. The missing values and gaps of some variables were filled with Python's Pandas tool using a linear interpolation method. To ensure that all the data was free of major outliers, Python's Zscore tool was used. This tool detects and removes the outliers by computing the value of a normal distribution over the standard deviation. By using a threshold of +/-2.5 for the standard deviation (including around 95% of the data) it could be ensured that the remaining data was clean enough for further statistical computations. By exporting all the variables as a single, gapless and cleaned file with similar sampling intervals, the data could be further processed and analysed in the program HydroClimATe.

HydroClimATe is an analysis toolkit provided by USGS (United States Geological Survey), which automates several methods such as standardization, detrending, regression and correlation, in order to assess relations between hydrologic and climatic sets of data (Dickinson et al., 2014). For a better comparison and more apparent results, every pre-processed data file was loaded into the program and detrended with the curve fitting tool, which computes residuals for a time series as the difference between a fitted polynomial (mostly linear) at the time t. These residuals were then standardized to achieve similar scales

in the y-axis of each data file. The proximate relations between the standardized data files could then be computed with linear regression and correlation tool of the program. This procedure enables to observe the effects of the value change of a predictor x on a predictand y and computes possible time lags between them.

The precipitation data was transformed into a cumulative rainfall departure (CRD). The concept of the CRD is used to evaluate the temporal correlation of rainfall with surfaces of water or ground water levels, which are cumulative variables (Weber & Stewart, 2004; Xu & van Tonder, 2001).

The CRD is used as an estimation of the groundwater recharge and can be computed in the HydroClimAte tool kit. The transformation is performed by calculating the sum of the differences between the consecutive values of the initial precipitation data set and its mean value:

$$\sum (x_i - \bar{x})$$

Function 1

Where:

x_i = the value at time i

$\bar{x}$ = the mean of the time series

3.3 Modelling Recharge

The two recharge estimation models presented in this study showed to be applicable and well defined within regions that are similar or close to the study area. However, these approaches were slightly modified to work in the spatial resolution this study aims for and according to the availability of needed input data.

3.3.1 BALSEQ Model

This mathematical model is a lumped parameter approach, meaning it simplifies the physical manners of a spatially distributed system into topological defined structure that describes and approximates the reality under certain assumptions and hypothesis.

The model computes the soil moisture (SM) and the resulting deep recharge (R) by using daily data of rainfall (P in mm), potential evapotranspiration (PET in mm) and the constant variables Soil Conservation Service Curve Number (CN) and the water capacity of the saturated zone (AGUT in mm), which depend on the local geology (Ferreira, 1981; Ferreira & Rodrigues, 1988; Martins et al., 2021). The main computation of the recharge is based on the simple assumption of the balanced interaction between the input variables (Choudri, 2004) and can be described with the formula:

$$Soil\ Moisture\ (SM) = Precipitation\ (P) - Runoff\ (F) - Acutual\ Evapotranspiration\ (AET)$$

Function 2

The calculation of the Runoff is based on the method developed by the United State Soil Conservation Service (Soil Survey Staff, 2014), which uses the CN constant that has been described to be 72 in (Ferreira & Rodrigues, 1988) and 81 in (Martins et al., 2021) for the soil of the study area. The simplified formula for the runoff is:

$$F = \frac{25.4\ \left(P_s - \frac{200}{CN} + \right)^2}{\frac{P_s}{25.4} + \frac{800}{CN} - 8}\ (mm)$$

Function 3

Where P_s is the precipitation during a storm day. This initial loss of precipitation permits saturation of the surface layer of the soil. However, it only applies for storms whose precipitation exceeds the surface occupation of the soil (Ferreira & Rodrigues, 1988). This minimum limit of precipitation for the occurrence of runoff is applied to the model as a function of CN:

$$P_s = P > \frac{5080}{CN} - 50.8\ (mm)$$

Function 4

With this runoff value, the soil infiltration (I_s) was calculated as the difference between P and F. The soil infiltration is needed to transform the potential evapotranspiration into actual evapotranspiration (AET) as it determines the available water in the unsaturated zone.

The relationship between soil infiltration, potential evapotranspiration and actual evapotranspiration is described in (Martins et al., 2021) with the If-Else:

$$IF\ (I_s) < (PET)\ then\ (AET) =\ (I_s), else\ (AET) = (PET)$$

Function 5

This daily approach of estimating the actual evapotranspiration ignores the availability of water within the soil moisture storage of the prior days, meaning after a day of high precipitation the actual evapotranspiration is 0 if there is no rainfall at the current day, although the soil moisture store is filled to its maximum capacity.

A different approach to transform PET to AET, is presented in (Lima, 2020). Here daily water budget is computed as in function (1) with PET instead of AET. The resulting potential loss (L) which only occurs on days of negative values of the water budget can then be computed as a sum of the potential water budget from day x and its previous day. A potential soil moisture storage of this model is then determined by the AGUT value for days of no potential loss and for days with occurring L by the function:

$$AGUT\ \times e\left(\frac{L}{AGUT}\right)$$

Function 6

When the difference soil moisture storage of the day x and its previous day is zero or positive, the actual evapotranspiration is equal to the potential evapotranspiration. On days where this difference is negative, the AET is equal to the precipitation of that day minus that negative value.

With all variables given for function (2), the soil moisture and the recharge can be computed as the deep recharge which only occurs if SM exceeds its capacity (AGUT), which was defined to be between 100 and 143 in prior studies in this region (Ferreira & Rodrigues, 1988; Martins et al., 2021) :

$$IF\ (SM) < (AGUT)\ then\ (R) = (SM) - (AGUT), and\ (SM) = (AGUT)$$

Function 7

The actual value of the soil moisture and the recharge for a specific day can be computed as the cumulative sum of daily values under the consideration of the aforementioned functions and conditions. Under the assumption that the ERA5 data shows an accurate spatial distribution of the climate variables, meaning that all observation points and the DRAP Algarve weather station are within a region of very low spatial variability of the climate variables, the computation for this model is based on the values given by the DRAP Algarve weather station.

For calibration purposes of the model, the starting date was set 2 weeks prior to the starting date of the field measurements, in order to estimate the volume of water content in the vadose zone based on the climate drivers rather than setting this value to zero or estimating numbers of best fit.

3.3.2 LUMPREM Model

LUMPREM is also a lumped parameter model. This model simulates the water movement within the unsaturated zone. By using daily rainfall, potential evapotranspiration and site-specific defined variables such as irrigation, soil moisture storage and several earth properties attributes, LUMPREM computes time series of simulated groundwater recharge (Doherty, 2020).

The model uses a subroutine called RECHMOD which computes the zone occupied by plant roots, which therefore is affected by evapotranspiration processes, and defines the soil moisture storage (Figure 4). The balance equation adds water as rainfall and water loss in form of vegetative extraction (evapotranspiration), direct drainage (deep recharge) and macropore drainage (runoff), with the latter only being able to occur with a filled storage.

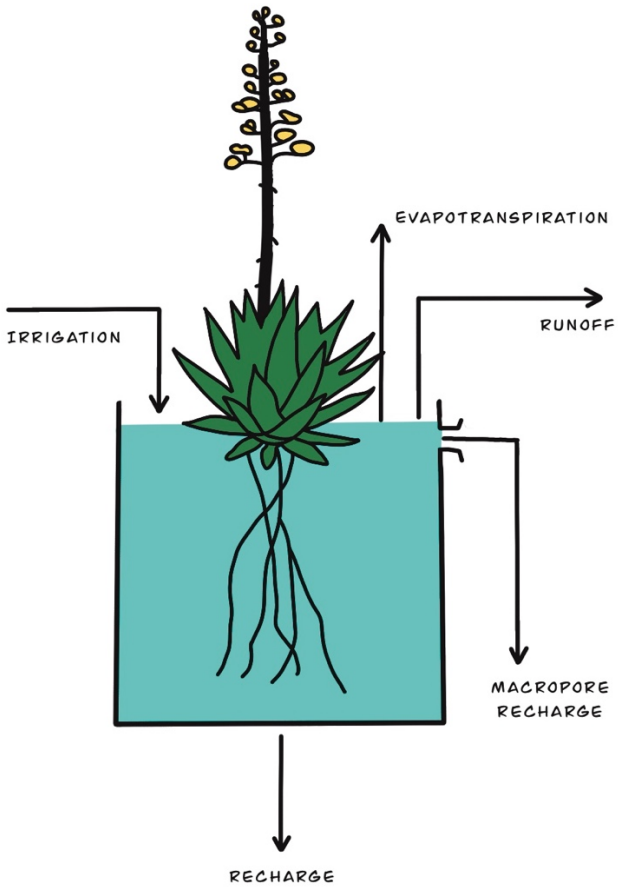

Figure 4: Sketch of the conceptual bucket model the LUMPREM model follows to simulate recharge.

The volume of the soil moisture store can be roughly estimated multiplying the depth of the root zone, which is commonly around 1m-2m, with the soil porosity within this zone, which is dependent of the regional geology and was estimated to be between 0.05 and 0.4 according to (de Castro et al., 2014) for the semi-karstic lime/sandstone medium of the study area. However, this value needs to be adjusted in the cases of deeper aquifers, as the overlying aquifer has the same effect as a larger soil moisture storage.

While the model directly uses the daily input sequences of precipitation, the daily input sequences of the potential evapotranspiration is transformed within the model to actual evapotranspiration. Due the evapotranspiration's dependency of the soil moisture (the less water in the root zone, the more the water is held more tightly by the soil). The rate of actual evapotranspiration is calculated within the model with the equation:

$$E = f\ E_p\ \times \frac{1 - e^{-\gamma v\prime}}{1 - e^{-\gamma} + e^{-\gamma v\prime}}$$

Function 8

Where:

E = actual evapotranspiration

E_p = potential evapotranspiration

f = "crop factor"

v' = relative volume of the soil moisture

γ = a constant dependent of the relationship between actual evapotranspiration and the soil moisture storage

The recharge occurs as a continuous unsaturated downward flow to the aquifer below the root zone. The rate of the recharge is dependent on the current volume stored in the unsaturated zone and the hydraulic conductivity which decreases with a decrease of saturation. The model computes the recharge according to the equation defined after (van Genuchten, 1980) with a pore-connectivity (l) of 0.5 for most soils according to (Mualem, 1976):

$$R = K_s\,[v']^l[1 - ([v']^{lm})^m]^2$$

Function 9

Where:

R = recharge

K_s = fully saturated hydraulic conductivity

v' = relative volume of the soil moisture

l = pore-connectivity parameter

m = constant determined by relationship between drainage rate and water storage

The computed recharge is not added to the aquifer simulation immediately, as the draining water suffers from a delay, which depends on the depth of the hydraulic head and transmissivity between the unsaturated zone and the aquifer. This lag is supplied in days.

The last components of the LUMPREM water balance macropore recharge and runoff only occur in heavy rain events or rain events with a fully saturated root zone. The amount of overflow is partitioned between macropore recharge and runoff.

By continuously calculating and updating the volume of the water in the soil moisture storage, LUMPREM simulates an elevation time series which is calibrated to the best fit to the measurements by mathematically adjusting the simulated curve with several factors and offset variables within the formula:

$$h = a + f_1 v + f_1 v^p$$

Function 10

Where:

h = the elevation

v = volume of the water in the RECHMOD container

a = the offset

f_1 = transform factor 1

f_2 = transform factor 2

p = is the power factor

Each observation site was simulated by one LUMPREM model. The variables of the input files of each model were manually calibrated to reach the highest correlation between the modelled and observed piezometric levels (Table 3). Each variable was selected by running the Pearson- and Spearman test between the modelled and measure waterheads after each adjustment until all tests showed the highest correlation. In some cases, adjustments of best correlation led to very low or even no recharge in the simulation, in these cases the lower correlation was considered before decreasing or losing recharge estimations.

Table 3: Input parameters for the LUMPREM models of each site, listing the variables that lead to the ground water head simulation with the best fit to the observations.

LUMPREM Input Variable	Description	610/180	610/179	606/1026	606/1461	606/1050
maxvol	Total volume of soil moisture store	0.28	1.1	1	2.5	0.8
irrigvolfrac	Fraction of irrigation (unactive = 0)	0	0	0	0	0
rdelay	Days between rain and recharge	0.2	0.2	0.2	0.2	0.2
mdelay	Days between rain and macropore recharge	0.1	0.1	0.1	0.1	0.1
ks	Saturated hydraulic conductivity	6	0.1	3	10	0.6
m	Shape between drainage rate stored water function	0.04	0.5	0.25	0.3	0.32
l	Shape between drainage rate and pore connectivity	0.5	1	0.5	0.5	0.6
mflowmax	Maximum volume of macropore recharge	0.1	0.1	0.1	0.1	0.1
offset	Offset factor for the pseudo-head	-4.5	0.2	-8	-7.4	-2
factor1	First factor for pseudo-head transformation	10	0.05	10	11	38
factor2	Second factor for pseudo-head transformation	4	1.5	0.5	0.5	2
power	Power of factor2 or pseudo-head transformation	1	1	1	1	2
surface	Topographic surface value for pseudo-head scaling	0	0	0	0	0
vol	Starting volume of soil moisture	0.15	0.1	0.27	0.1	0.21
nrbuf	Array for recharge travel delay	1	1	1	1	1
nmbuf	Array for macropore recharge delay	1	1	1	1	1

4 RESULTS

4.1 Piezometric Records

The GWL fluctuation at each site can be visualised by comparing the measurements inside a boxplot (Figure 5). The amplitudes of the piezometric levels seem to gradually increase with the sites' distance to the Ocean (the further North, the larger the amplitude). With a maximum amplitude of 0.5 m, the most southern station (610/179), which recorded the GWL slightly above mean sea level, has the smallest range of fluctuations. The sites 610/180, 606/1026, and 606/1462, have measured groundwater levels in comparable depths (all below the mean sea level), maximum amplitudes of 2 m, 3 m and 5 m, respectively. The northernmost site (606/1050), which measures GWLs at the greatest elevation above mean sea level, recorded the largest fluctuations, with a maximum amplitude of 6 m.

Throughout the observation period, all measurements show a rise in the piezometric level until mid-March, where the trend becomes negative. While site 610/180 and 606/1050 show higher variations in the trends with more increasing, constant and decreasing periods of different intensities (Figure 6 and 10), 610/179, 606/1462 and 606/1026 only show increases of the piezometric measurements (Figure 7,8 and 9). All significant increases of each plot seem to occur during the same or a similar time window.

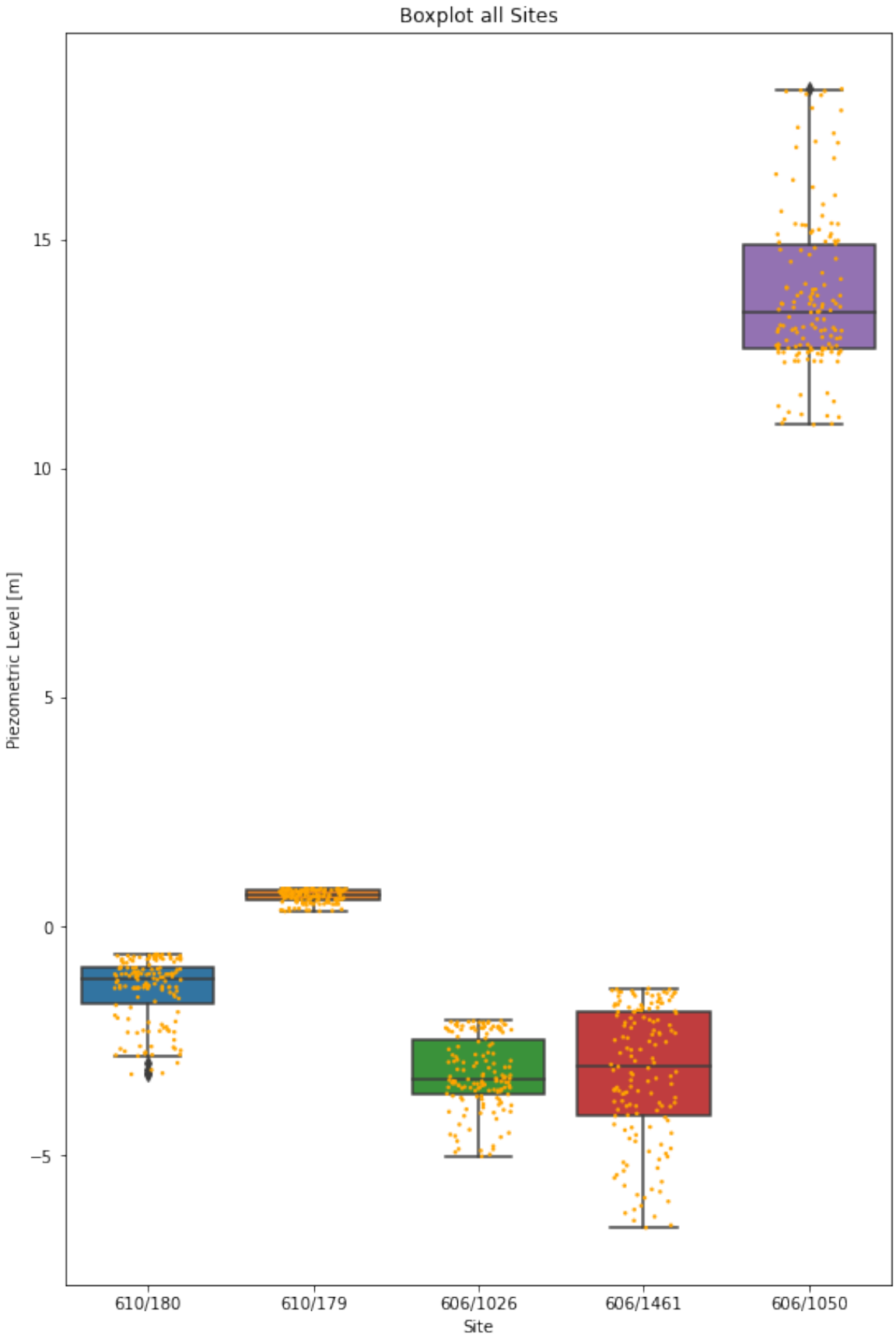

Figure 5: Boxplot comparison of all measured piezometric levels, showing range and level of the measurements and distribution of each data set as orange jitter points.

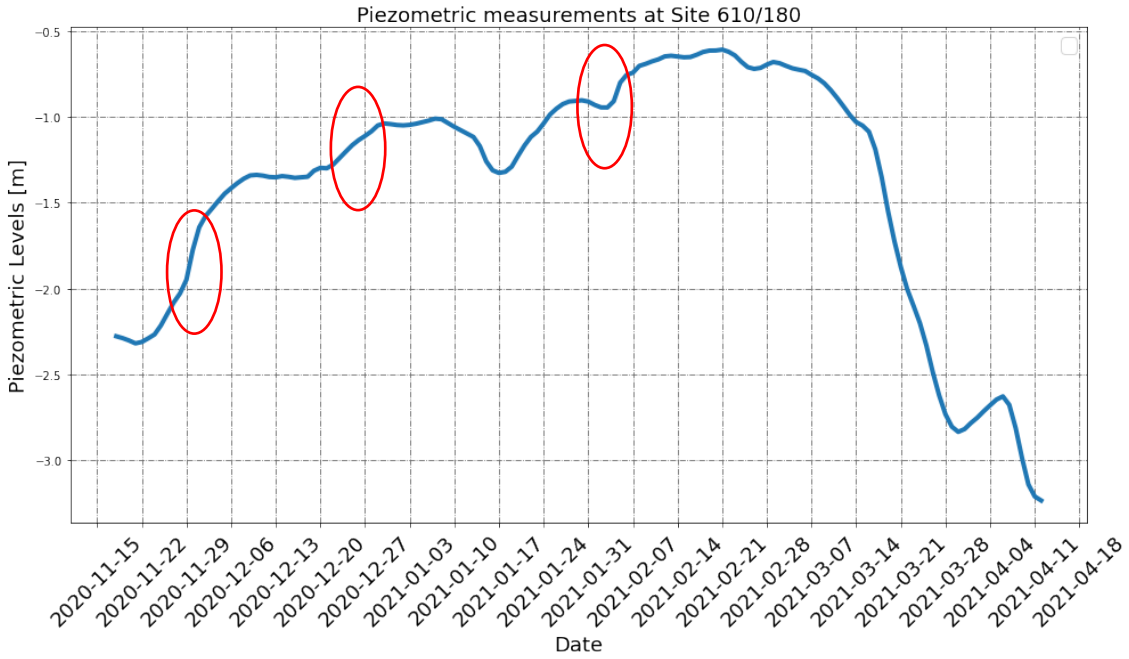

Figure 6: Daily piezometric measurements [m] of site 610/180 from 18. November 2020 to 12. April 21. The red circles mark the significant rises, which occur at most of the sites during the same time window.

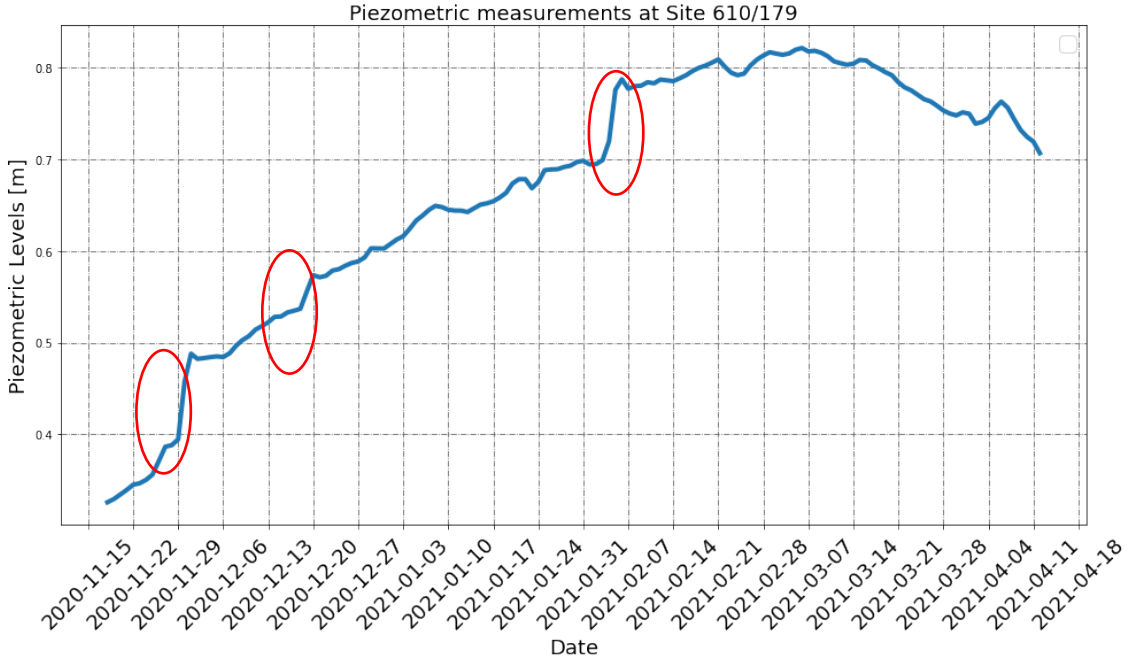

Figure 7: Daily piezometric measurements [m] of site 610/179 from 18. November 2020 to 12. April 21. The red circles mark the significant rises, which occur at most of the sites during the same time window.

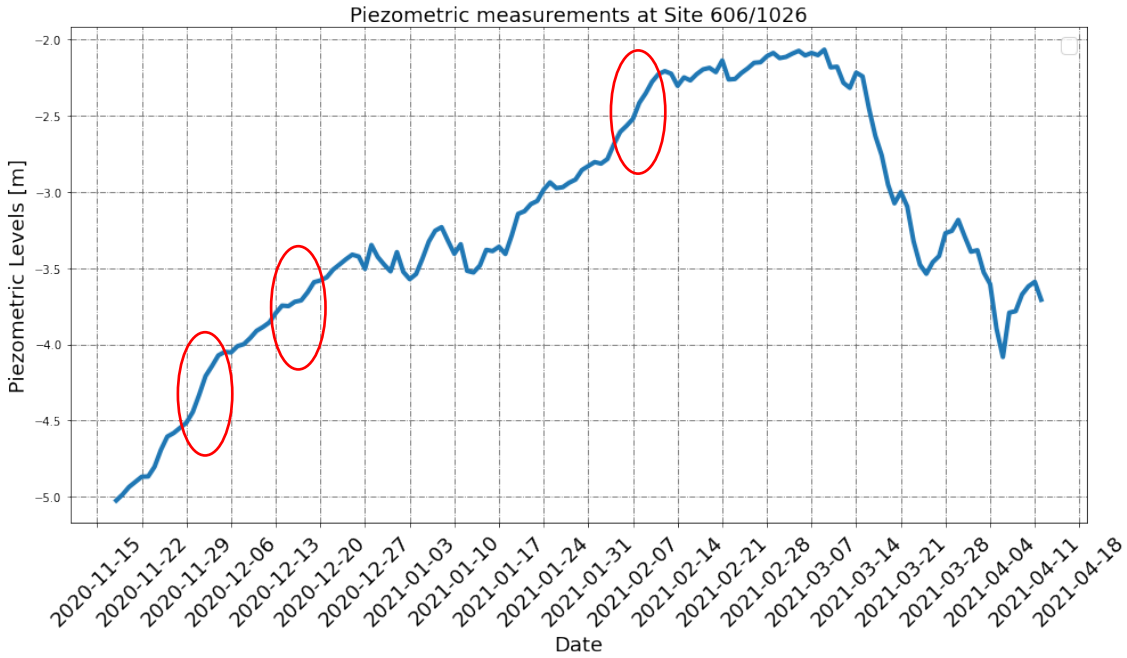

Figure 8: Daily piezometric measurements [m] of site 606/1026 from 18. November 2020 to 12. April 21. The red circles mark the significant rises, which occur at most of the sites during the same time window.

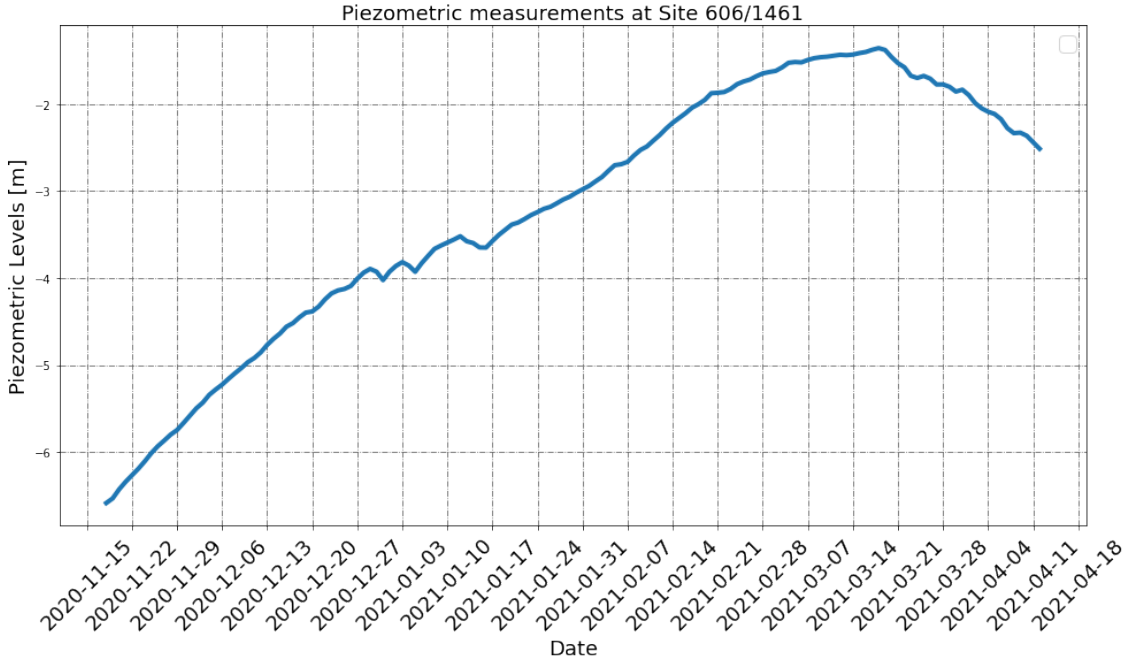

Figure 9: Daily piezometric measurements [m] of site 606/1461 from 18. November 2020 to 12. April 21, showing an overall gradual rise, without significant events.

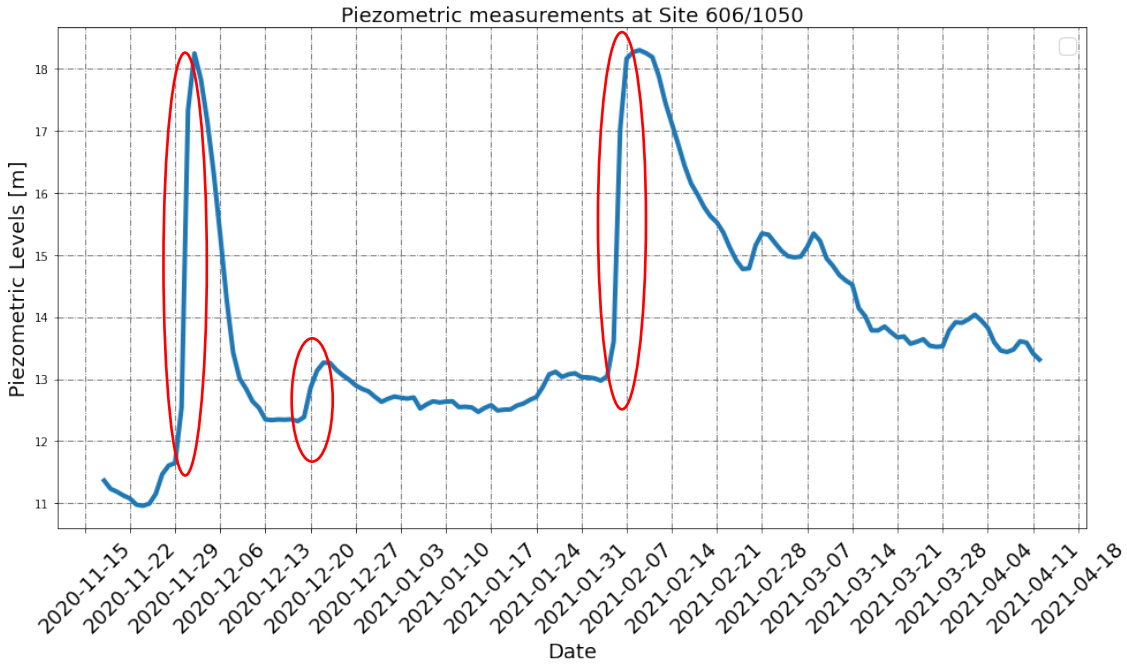

Figure 10: Daily piezometric measurements [m] of site 606/1050 from 18. November 2020 to 12. April 21. With very extreme rises marked by red circles, which immediately recover into more stable records. The rises occur at similar time windows as observed at other sites.

4.2 Climate Data

The comparison of the climate data from the DRAP Algarve weather station and the ERA5 reanalysis show big differences in the amplitudes of the rainfall events (Figure 11). Although the ERA5 data seems not to represent the actual measurements very well, the temporal distribution of significant rain events is accurate (Belo-Pereira et al., 2011). Both data sets have their maximum daily rainfall during the beginning of February. While the weather station records a maximum of 73.2 mm during this period, the ERA5 reanalysis data only reaches a max. of 24.9 mm. The recorded sum of mm of rain during the observation period is 409.8 mm according to the weather station and 127.5 according to the reanalysis data.

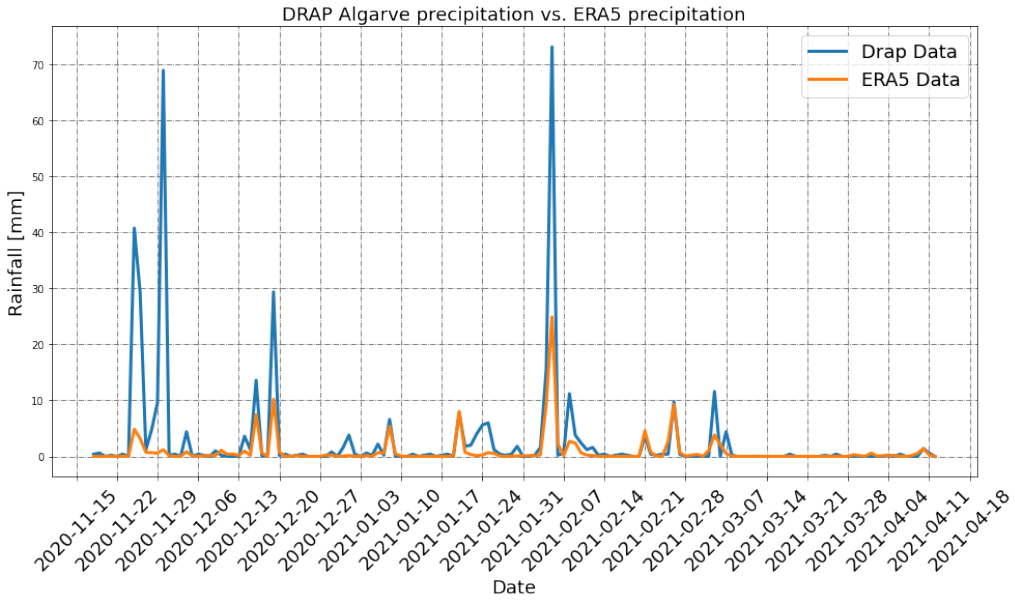

Figure 11: Comparison of recorded precipitation of the DRAP Algarve weather station (orange graph) and the ERA5 reanalysis data (blue graph) over the period between 18. November 2020 to 12. April 2021.

The comparison between the temperature records of the two different derived data sets show more similarities (Figure12). Both show a very similar trend with peaks during the same periods. The weather station shows a temperature maximum of 18.8°C during end of March and a minimum of 4.7°C around the 10. of January. The ERA5 data set recorded maximum and minimum are during the same time periods with 18.6°C and 4.5°C. The temperature mean recorded by the weather station over the observation period is 12.8° C and 12.6°C recorded by ERA5.

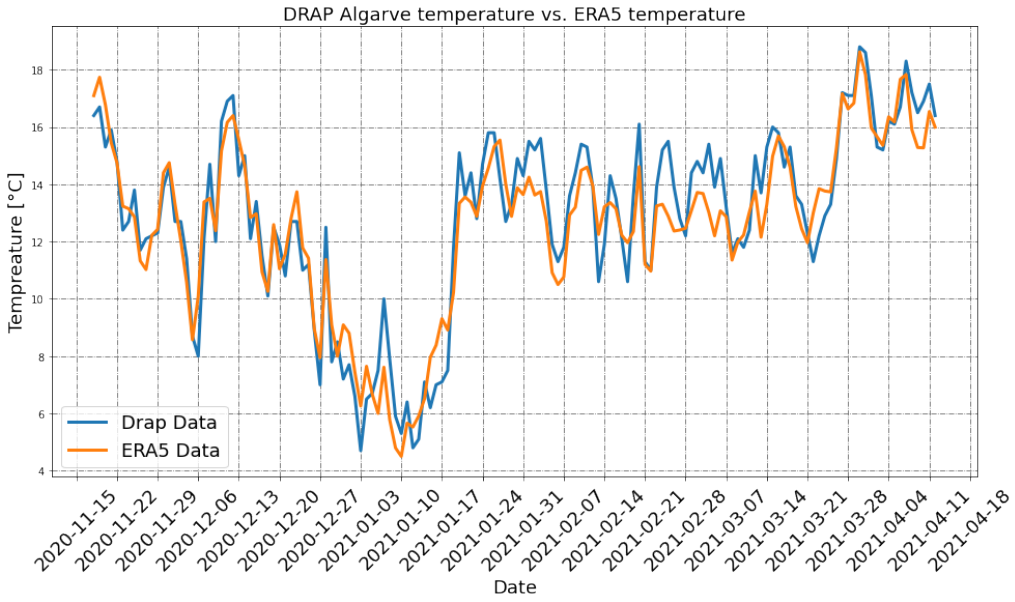

Figure 12: Comparison of recorded temperatures of the DRAP Algarve weather station (1.5m above ground, orange graph) and the ERA5 reanalysis data (2m above ground, blue graph) over the period between 18. November 2020 to 12. April 2021.

The ERA5 grid mainly covers the study area with 4 pixels (A, B, C, D). The extracted and over time interpolated data sets of each pixel show that there is very low to no variability within these spatial ranges (Figure 13 & 14). Pixels A and D show less variabilities within the extracted data than pixels A and B, especially regarding the temperature (Figure 15).

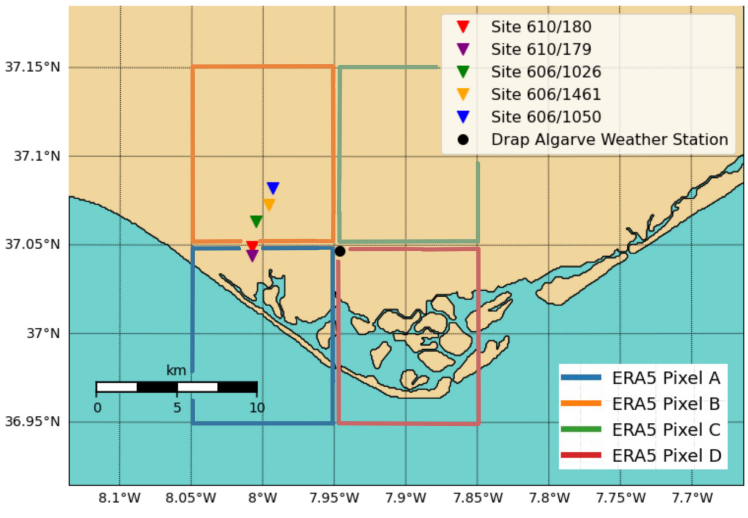

	Site covered	Longitude Range	Latitude Range
Pixel A	610/180 610/179	36°95' – 37°05'	-8°05' – -7°95'
Pixel B	606/1026 606/1461 606/1050	37°05' – 37°15'	-8°05' – -7°95'
Pixel C	Area above weather station	37°05' – 37°15'	-7°95' – -7°85'
Pixel D	Weather Station	36°95' – 37°05'	-7°95' – -7°85'

Figure 13: Map showing the 4 pixels of the ERA5 data covering the study site and table listing each pixel, their coordinates and the features covered (Pixel A blue square, Pixel B orange square, Pixel C green square, Pixel D square).

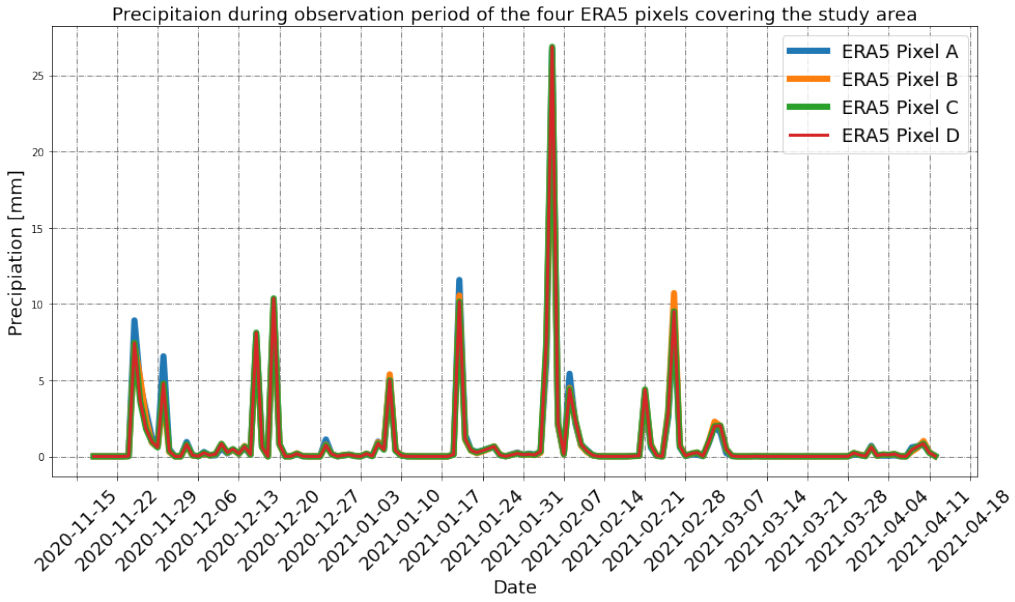

	Pixel A	Pixel B	Pixel C	Pixel D
MAX	26.67 mm	26.86 mm	25.51 mm	26.86 mm
MEAN	0.98 mm	0.95 mm	0.95 mm	0.95 mm
SUM	143.86 mm	138.75 mm	139.06 mm	138.75 mm

Figure 14: Comparison of the four precipitation time series extracted from the 4 ERA5 pixels during the observation period and table showing the mean, max and sum recorded within each pixel (Pixel A blue graph, Pixel B orange graph, Pixel C green graph, Pixel D red graph), suggesting a low spatial variation of the rainfall within the area.

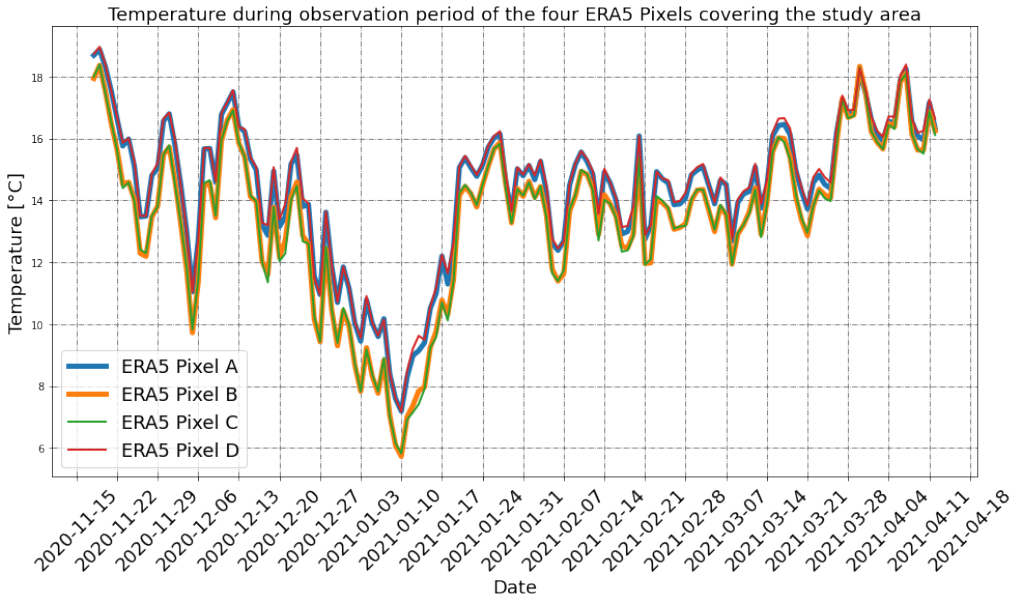

	Pixel A	Pixel B	Pixel C	Pixel D
MIN	7.2°C	5.8°C	5.7°C	7.2°C
MAX	18.8°C	18.4°C	18.4°C	19.0°C
MEAN	14.3°C	13.4°C	13.4°C	14.4°C

Figure 15: Comparison of the four temperature time series extracted from the 4 ERA5 pixels during the observation period and table (Pixel A blue graph, Pixel B orange graph, Pixel C green graph, Pixel D red graph). Showing the mean, max and sum recorded within each pixel, suggesting a low spatial variation of the temperature within the area.

The contour lines support the idea of a general very low variability of the climate drivers within in the study area and the main variability, especially for the temperature, being induced by longitudinal changes (Figure 16). All measuring sites and the DRAP Algarve weather station seem to be surrounded by a very similar climate setting, during the observation period and the period between June 2020 and September 2020 (Figure 17). During the period of the summer months, the precipitation shows to be close to 0 as expected and the spatial variability between both climate factors seems shift to a latitudinal dependency, with temperature increasing and the precipitation decreasing towards East.

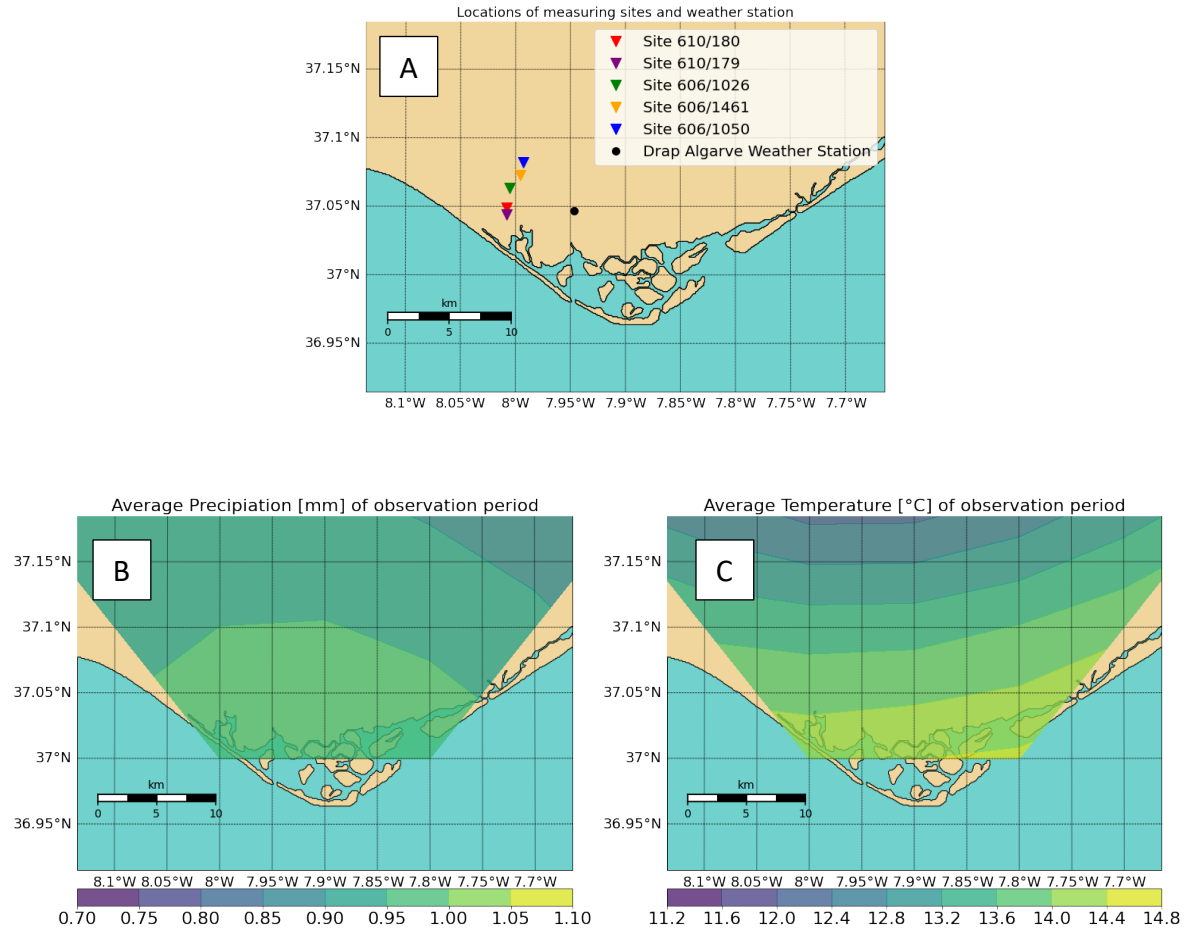

Figure 16: Comparison of spatial distribution of climate factors and sites of study area between 18.11.2020 and 12.04.2021. A) Map of study area and locations of all measuring sites and the DRAP Algarve weather station. B) Contour map showing the average precipitation [mm] during the observation period. C) Contour map showing the average temperature [°C] during the observation period.

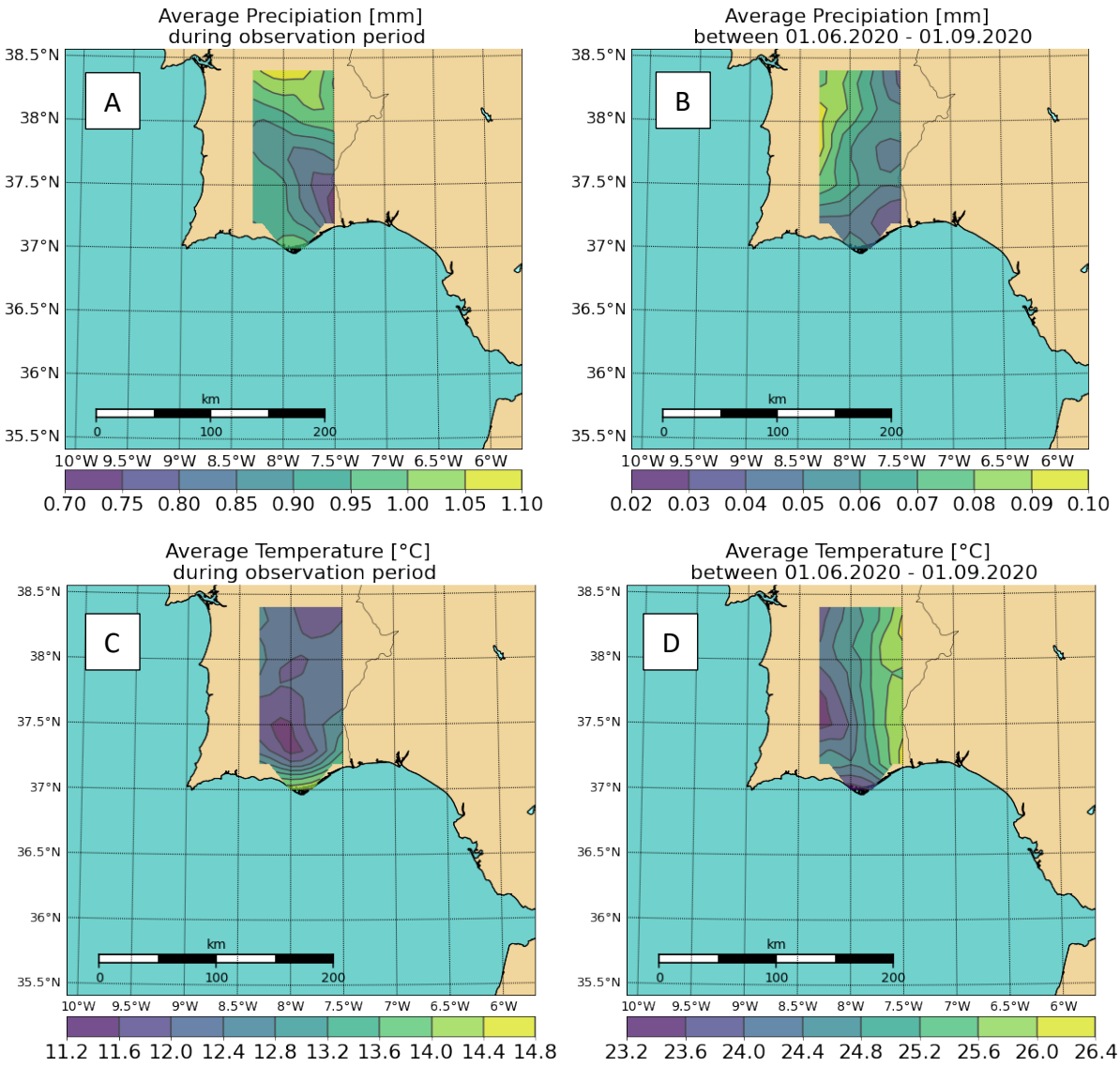

Figure 17: Contour maps comparing the shifts of the climate factors during the observation period and the summer months between 01.06.2020-01.09.2020. A) Contour map of average precipitation during the observation period. B) Contour map of average precipitation during the summer months. C) Contour map of average temperature during the observation period. D) Contour map of average temperature during the summer months.

Looking at the relationship between rainfall, temperature and the evapotranspiration clearly shows the dependency of the evapotranspiration to the other two climate variables, as the potential evapotranspiration follows along with the trends of the temperature (Figure 18).

The two functions presented for the actual evapotranspiration calculation show very different outcomes (Figure 19). Both approaches attempt to add the effect of rainfall in terms of water available in the soil for the process. The rather simple approach of Martins et al. (2021, Function 5) leads to high differences between actual and potential evapotranspiration, simply because it ignores the available water within the soil moisture storage on days with no rainfall events (Figure 19). The approach of Lima (2020, Function 6), computes an actual evapotranspiration that closely resembles the potential evapotranspiration until a longer period without rainfall events, leading to a better representation of the reality as it includes the concept of the soil moisture.

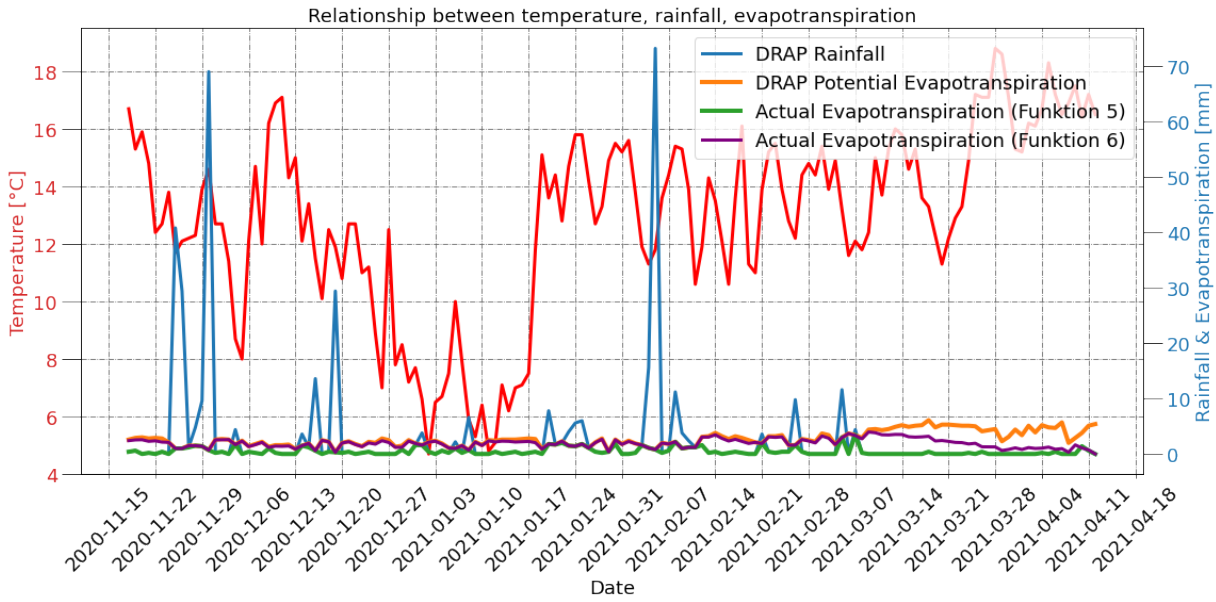

Figure 18: Time series comparison of the temperature (red graph), the rainfall (blue graph), the actual evapotranspiration according to function 5 (green graph) and the actual evapotranspiration according to function 6 (purple graph). Showing the dependency of the evapotranspiration processes to the climate drivers.

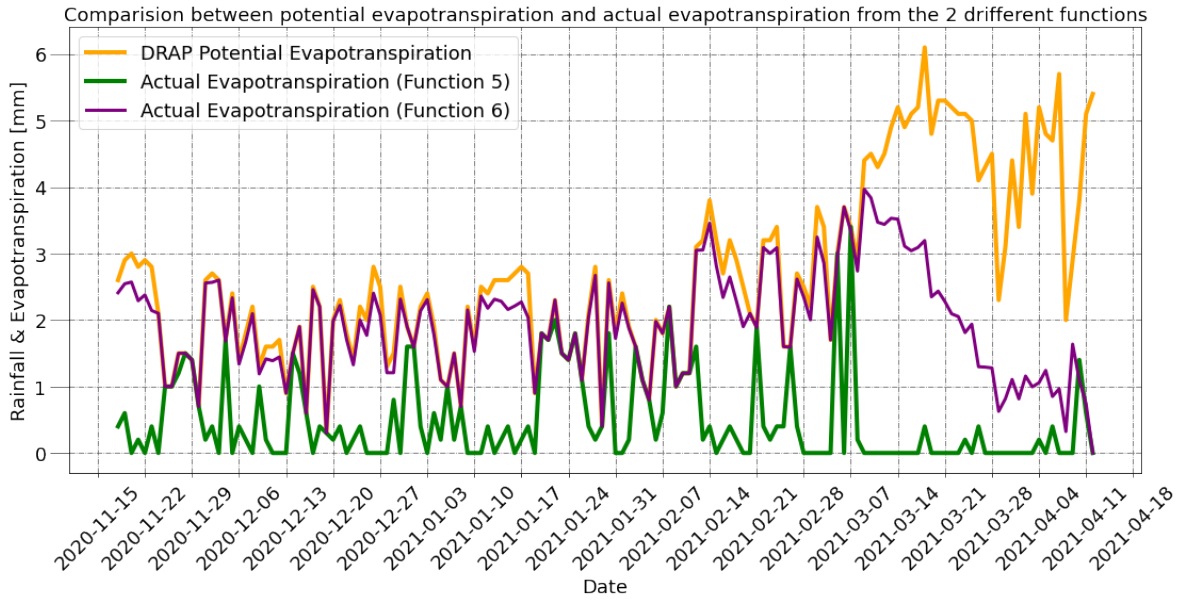

	Potential	Actual Function 5	Actual Function 6
MIN	0.30 mm	0.00 mm	0.00 mm
MAX	6.10 mm	3.40 mm	3.97 mm
MEAN	2.67 mm	0.47 mm	1.93 mm

Figure 19: Time series comparison of the potential evapotranspiration (orange graph) and the two different approaches to compute the actual evapotranspiration (function 5: green graph, function 6: purple graph), with table showing minimum mean and maximum of each graph.

4.3 Statistical Analysis

To visualize the statistical connection between the climate variables of temperature (T), precipitation (as cumulative rainfall departure, CRD), potential evapotranspiration (PET) and the five piezometric measurements (610/180, 610/179, 606/1026, 606/1461, 606/1050), the pre-processed data files have been plotted as three heatmaps each having one of the climate variables as the correlating data set (Figure 20).

Rainfall (as CRD) is found to be strongly positive correlated with all piezometric measurements and slightly negative correlated with the other two climate variables. The correlation coefficient for the groundwater levels ranges from 0.72 for site 606/1050 to 0.83 for site 610/179 and is around -0.3 for T and PET. The heatmaps for temperature and potential evapotranspiration are very similar, both variables show to be negatively correlated with all groundwater measurements. The correlation coefficient between T and the piezometric measurements range from -0.015 for site 606/150 and -0.41 for site 610/179.

The correlation coefficient between PET and the piezometric measurements range from -0.13 for site 606/1050 to -0.42 for site 610/179.

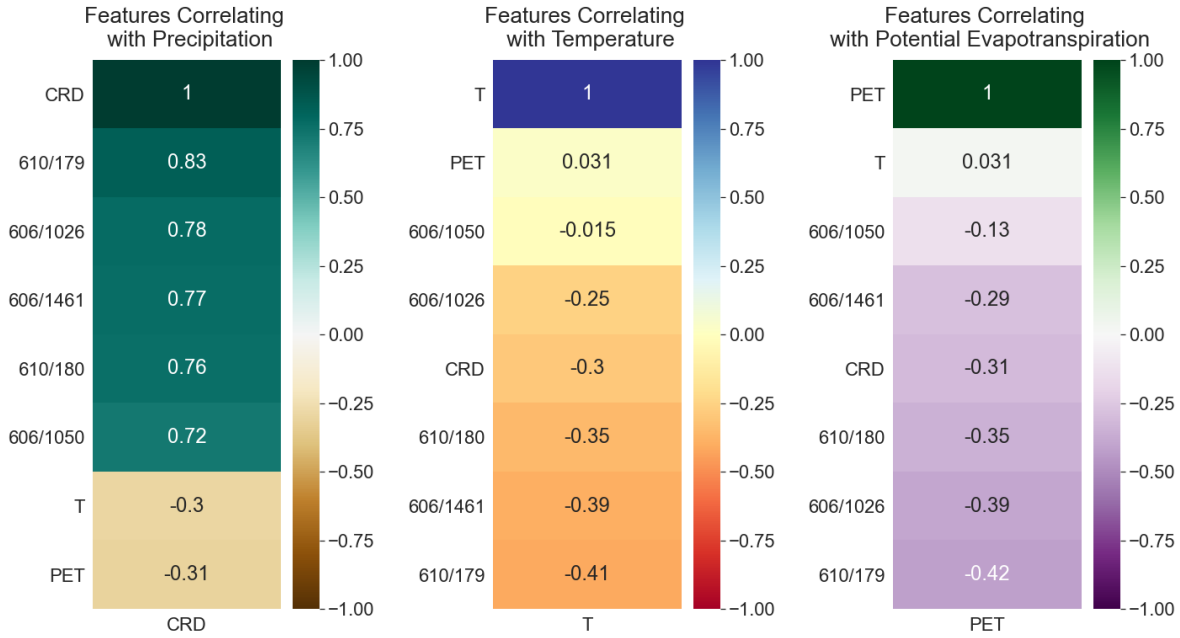

Figure 20: Heatmaps of the three climate variables CRD (left), T (middle) and PET (right), showing the correlation between each other and the piezometric measurements.

A scatter matrix including all pre-processed data files of the piezometric measurements, showing scatter plots and correlation coefficients between each measurement with a histogram of each data set, was created to show the relationships between each site (Figure 21). All measurements are positively correlated. While the sites within the Campina de Faro aquifer (610/180, 610/179, 606/1026, 606/1461) around 0.95, site 606/1050, which is in the São João da Venda-Quelfes, shows lower correlations, with coefficients between 0.39 and 0.52.

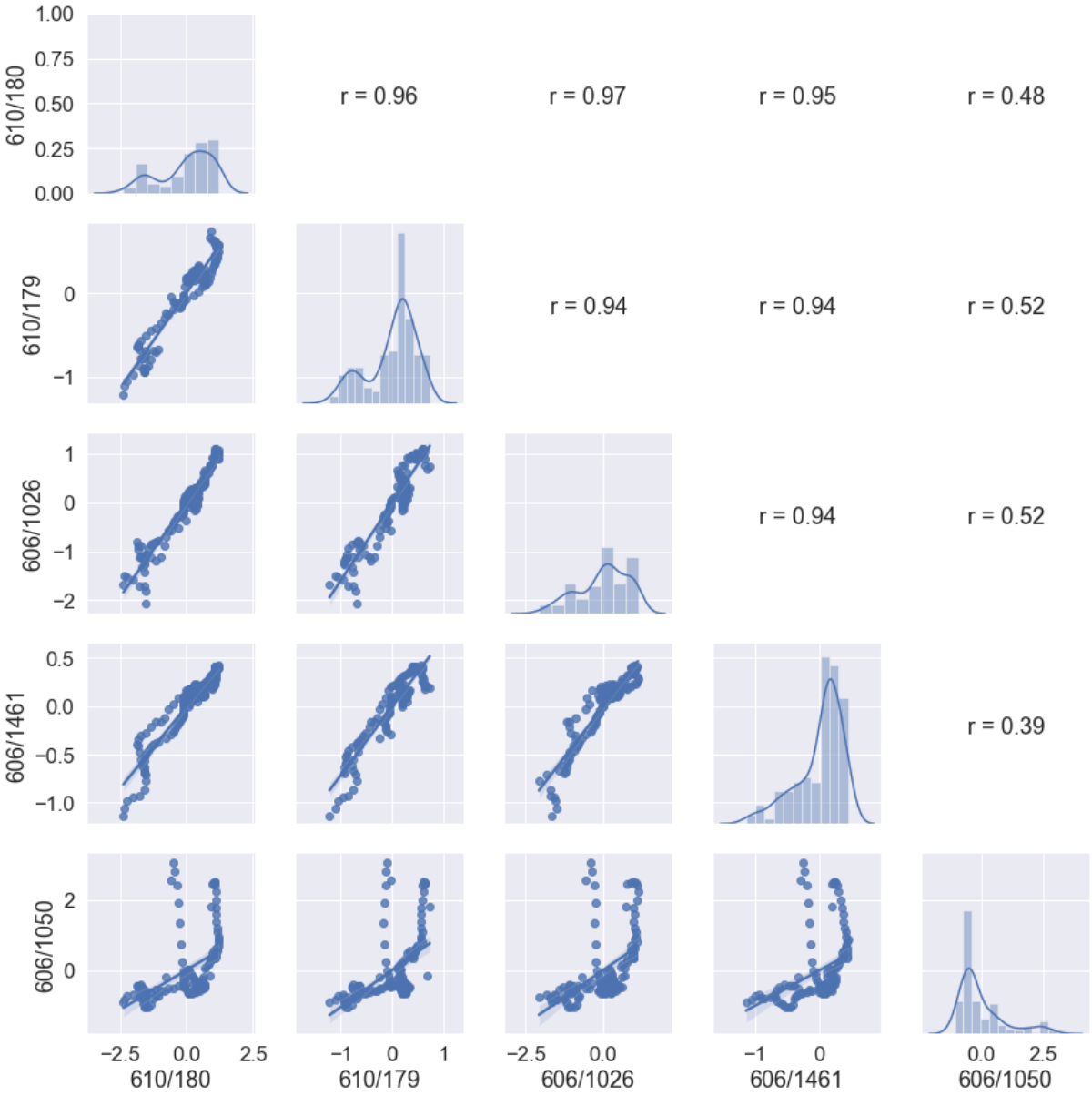

Figure 21: Scatter matrix including all pre-processed piezometric measurements, showing scatter plots between each measuring site, a histogram for each data set and the correlation coefficient between each site, indicating a generally high positive correlation between all measurements.

A cross- correlation computation was only conducted joining the cumulated rainfall departure and each measurement site, since the potential evapotranspiration and the temperature only affect the process of recharge, not the groundwater level itself (Figure 22). This computation included only positive correlation and maximum lag of 30 days as no higher lags were to be expected, confirming the immediate response of the ground water levels with rainfall events by showing the maximum corelation, with coefficients around 0.75, occurring on day 0 within the cross-correlation plot.

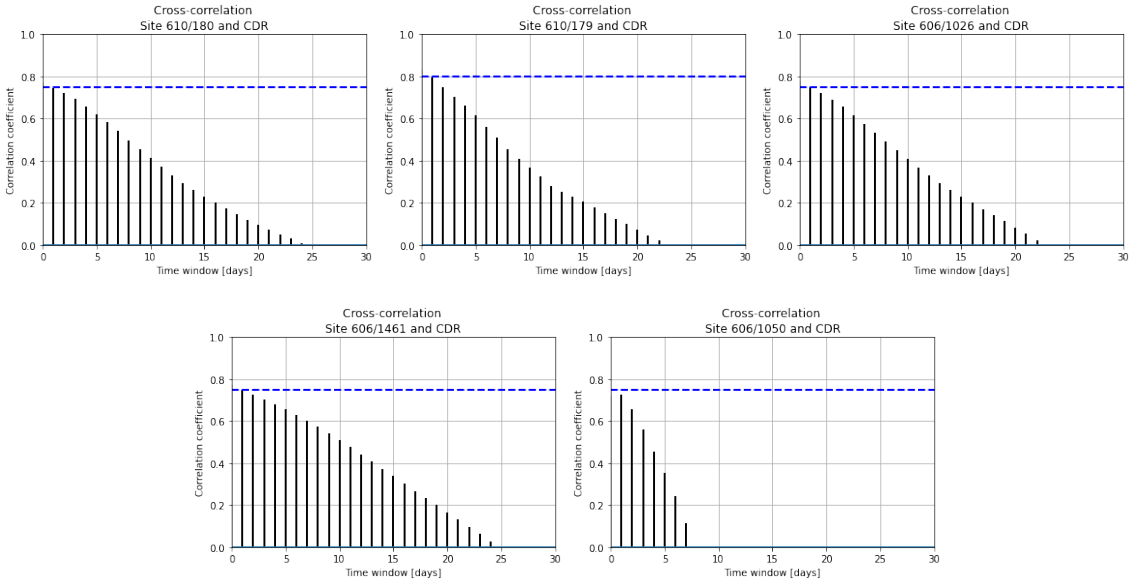

Figure 22: Cross-correlation plot joining the CRD with each piezometric measurement with a maximum lag window of 40 days and the maximum correlation within that window (blue line), indicating that the groundwater level at each site immediately responses to rainfall events.

4.4 BALSEQ Outputs

According to given variable within the literature, two different BALSEQ models have been calibrated. Model A follows the geological assumption of the hosting substrates composition, hydrological conductivity, and root depth for the study area, as described by Ferreira & Rodrigues (1988), with a CN value of 72 and AGUT value of 100. Model B follows the weighted approach of the parameters for the same location from Martins et al., (2021), with a CN value of 81 and AGUT value of 130.

The BALSEQ model in general computes a daily recharge that when plotted closely resembles the main peaks of the rainfall input data.

The simulated soil moisture storage of the unsaturated zone shows high variation throughout the model's running period, due to its sensibility to smaller amplitude climate forcing. The deep recharge graph (accumulated recharge) only shows an uprising trend within a few events, where the unsaturated zone reaches its maximum capacity (AGUT value), with the period of highest recharge occurring with the strongest rainfall event around the end of November. Since the model ignores any form of travel time of water through the system, the graph was smoothened with Savitzky-Golay filter (Chen et al., 2004), in order to represent a more realistic time series of this output variable. This smoothed graph of accumulated recharge then was correlated with the measured piezometric levels.

Model A (Figure 23 A) simulates a total recharge over the observation period of 160.32 mm and therefore actually replicates identical results as described in (Ferreira & Rodrigues, 1988). Model B (Figure 23 B) simulates a total recharge of 81.58 mm over the observation period. Each model's recharge and soil moisture has been correlated to the piezometric measurements in form of heatmaps (Figure 24), showing Model B generally reaches higher correlations with each site. The sites 610/179, 606/1026 and 606/1461 score very high correlation coefficients (above 0.8) with the smoothed recharge of both models. While sites 610/180 and 606/1050 in comparison show relatively low correlations with the recharge graph, these sites are the only features in the heatmaps that positively correlate with the soil moisture storage.

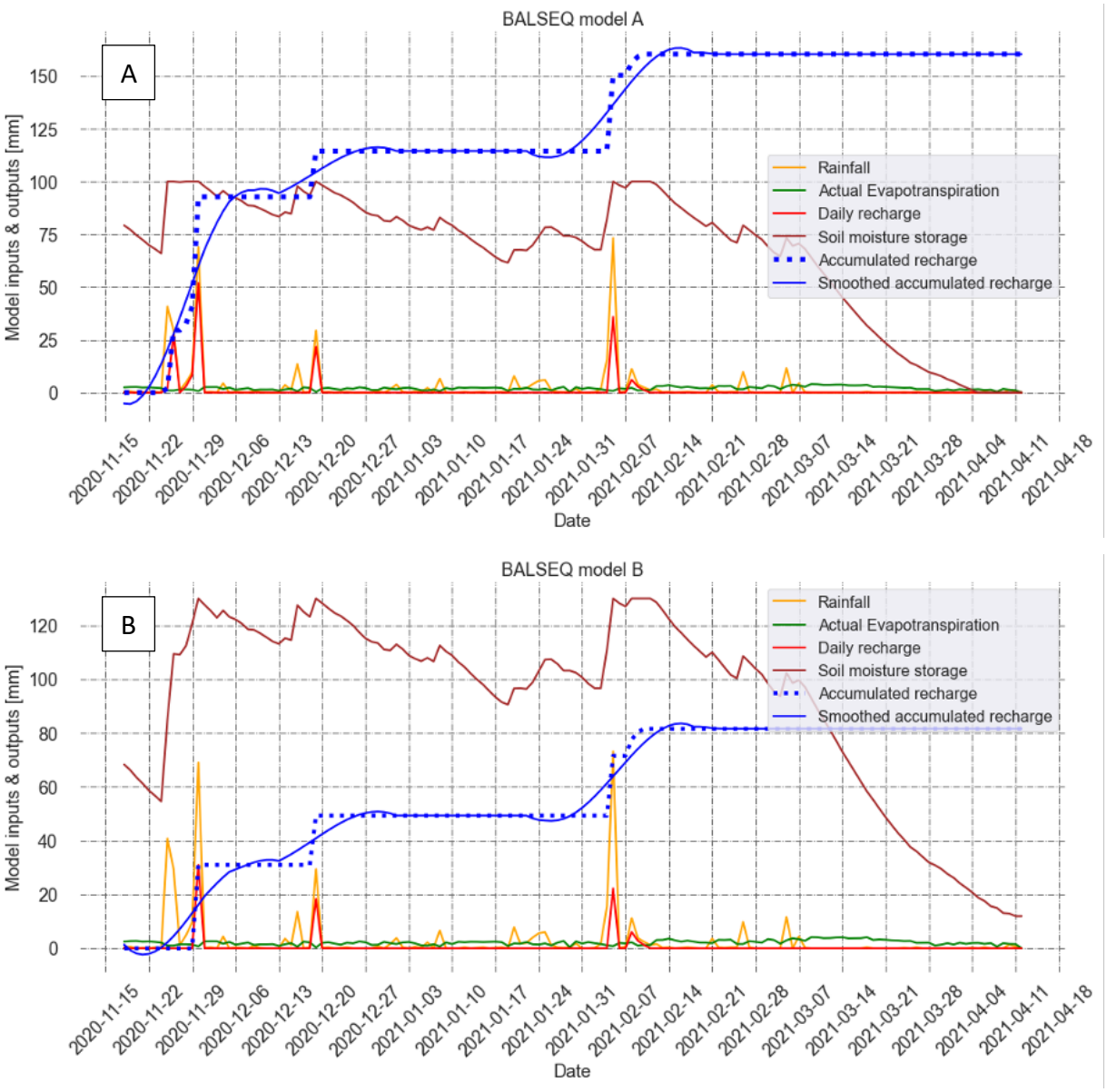

Figure 23: Comparison between BALSEQ model A and BALSEQ model B, showing rainfall (yellow graph), actual evapotranspiration (green graph), daily recharge (red graph), soil moisture storage (brown graph), accumulated recharge (blue, dashed graph) and smoothed accumulated recharge (blue graph). A) Model A simulating 5 recharge events, leading to a total recharge of 160.32 mm over the observation period. B) Model B, simulating 4 recharge events, leading to a total recharge of 81.58 mm over the observation period.

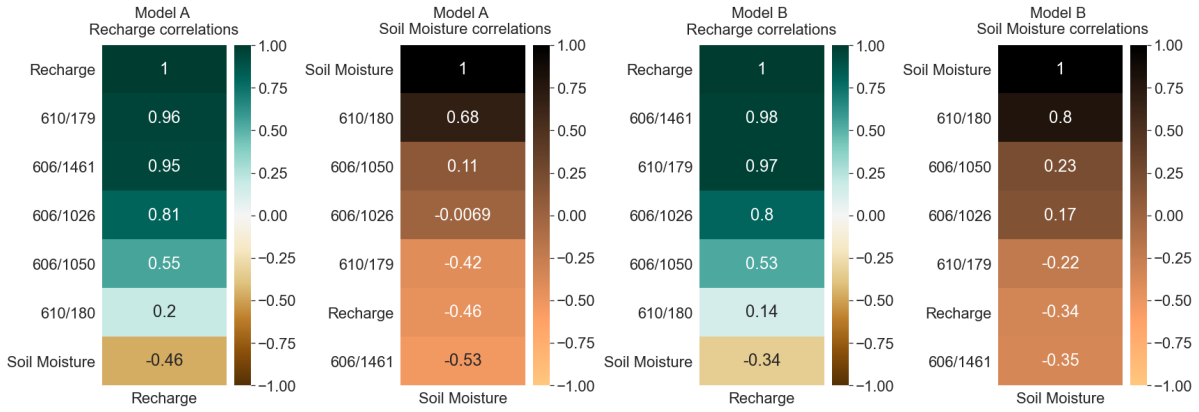

Figure 24: Heatmaps comparing the correlations of the BALSEQ model's simulated recharge with the measured piezometric levels (blue maps) and with the simulated soil moisture storage (brown maps), Model A (left) and Model B (right).

4.5 LUMPREM Outputs

The manually calibrated LUMPREM models generally lead to piezometric head simulations that highly correlated with the observation data (Figure 25-29). The models for the sites 610/179, 606/1026, and 606/1461 all have very high correlation coefficients, all above 0.92. Models for sites 610/180 and 606/1050, on the other hand, had slightly lower coefficients of 0.85 and 0.7, respectively. The calculated recharge strongly varies with each model and varies within its temporal occurrence through the observation period. Sites 610/180 and 606/1050, with a model recharge of 16.97 and 93.67 respectively, are the only simulation that show reasonable quantities of recharge within the first half of the observation period. The other models (610/179, 606/1026 and 606/1461) suggest that the main recharge at the location only occur with the last major rainfall events within the time frame, with major peaks of recharge around February. Despite the high correlation coefficients between simulation and observation at site 606/1461, the model's extremely low recharge value suggests a calibration failure.

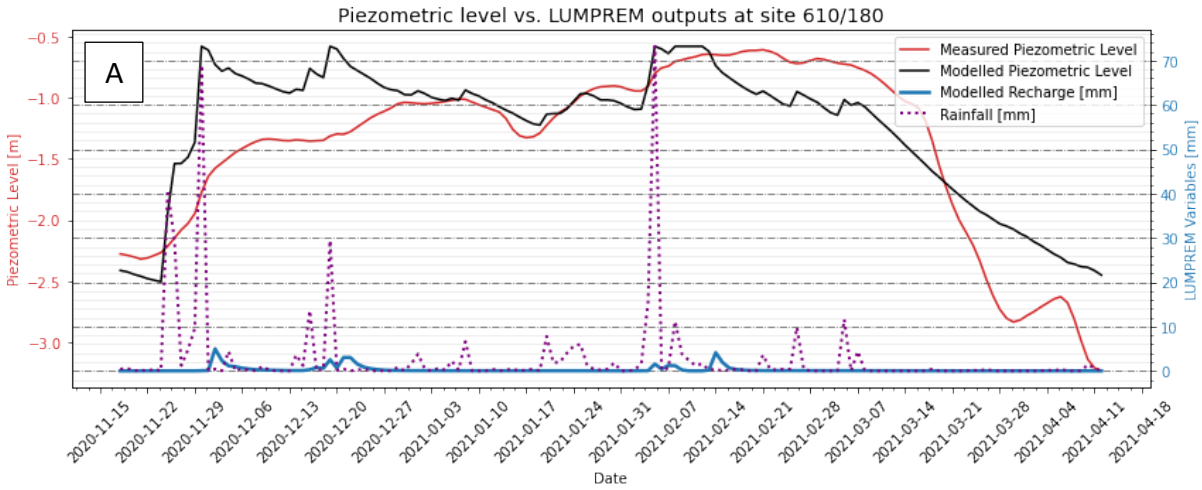

B	Measured Piezometric Level [m]	Modelled Piezometric Level [m]	Recharge [mm]
MAX	-0.61	-0.58	4.97
MIN	-3.23	-2.5	0
MEAN	-1.39	-1.25	0.27
SUM	-	-	39.43
Pearson-Test	r-value:0.8506 p-value:4.8334e-42		
Spearman-Test	r-value:0.5403 p-value:1.93821e-12		

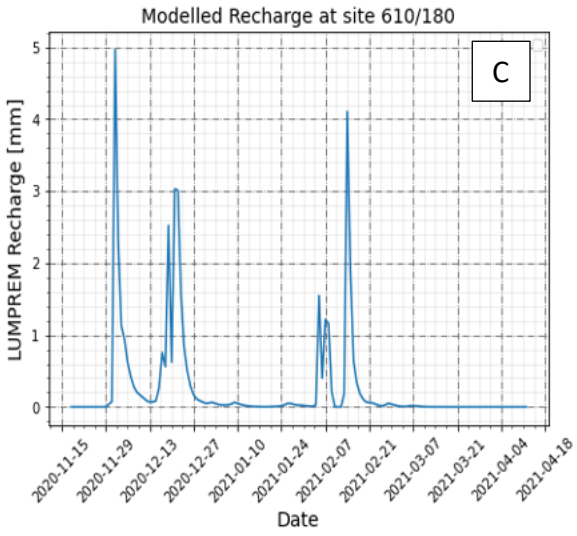

Figure 25: LUMPREM model results and comparison to field measurements at site 610/180. A) Timeseries comparison between modelled (black line) and observed piezometric level (red line), including the rainfall input data (dashed purple line) and modelled recharge (blue line). B) Table comparing the attributes of the two time series, showing maximum, minimum and mean values of the modelled and observed data, the sum of the modelled recharge as well as the Pearson and Spearman correlations of the two time series. C) Scaled modelled recharge plot, showing the distribution of the recharge events over the observation period (blue line).

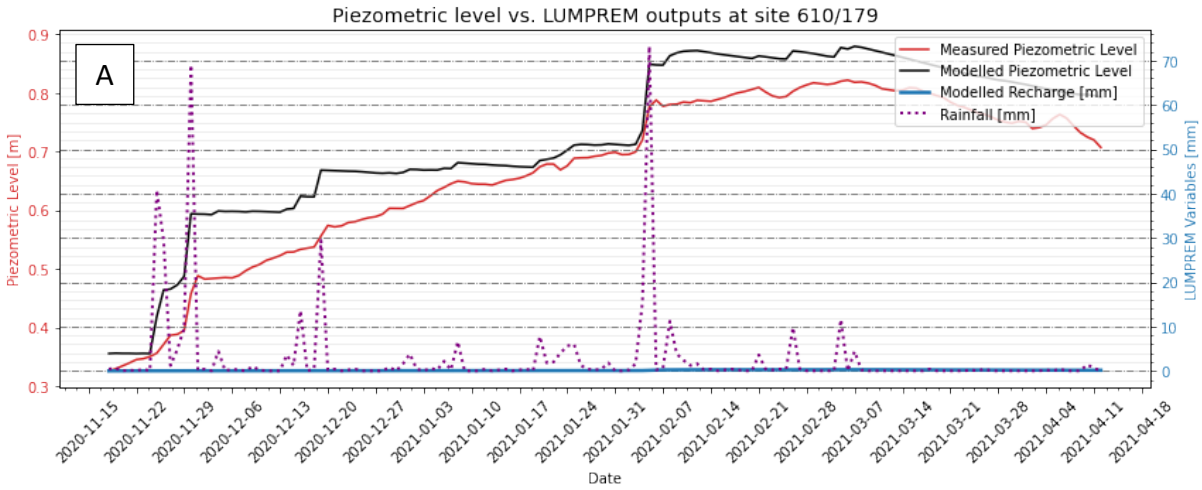

B	Measured Piezometric Level [m]	Modelled Piezometric Level [m]	Recharge [mm]
MAX	0.82	0.88	0.27
MIN	0.33	0.36	0
MEAN	0.67	0.72	0.12
SUM	–	–	16.97
Pearson-Test	r-value:0.9795 p-value: 3.9083e-102		
Spearman-Test	r-value: 0.9795 p-value: 3.9083e-102		

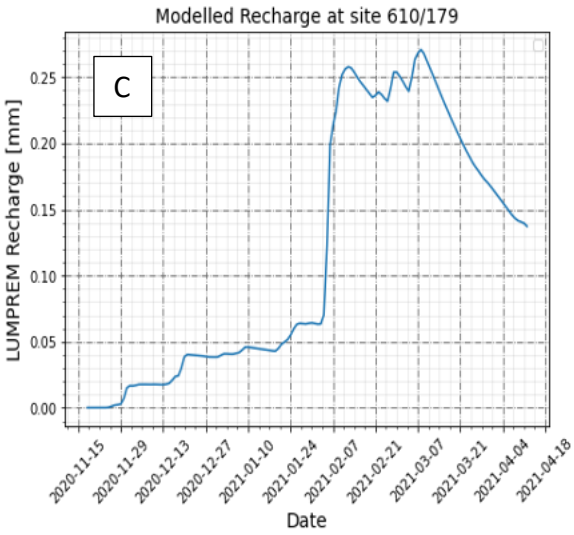

Figure 26: LUMPREM model results and comparison to field measurements at site 610/179. A) Timeseries comparison between modelled (black line) and observed piezometric level (red line), including the rainfall input data (dashed purple line) and modelled recharge (blue line). B) Table comparing the attributes of the two time series, showing maximum, minimum and mean values of the modelled and observed data, the sum of the modelled recharge as well as the Pearson and Spearman correlations of the two time series. C) Scaled modelled recharge plot, showing the distribution of the recharge events over the observation period (blue line).

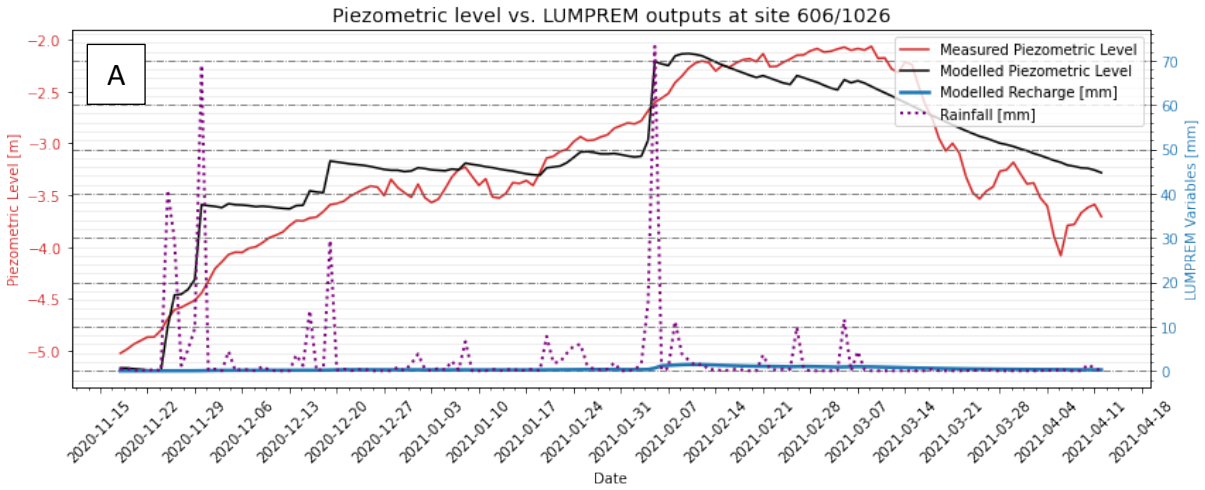

B	Measured Piezometric Level [m]	Modelled Piezometric Level [m]	Recharge [mm]
MAX	-2.06	-2.13	1.43
MIN	-5.03	-5.19	0
MEAN	-3.22	-3.13	0.44
SUM	-	-	64.84
Pearson-Test	r-value: 0.9259 p-value: 8.7261e-63		
Spearman-Test	r-value: 0.8899 p-value: 8.7261e-63		

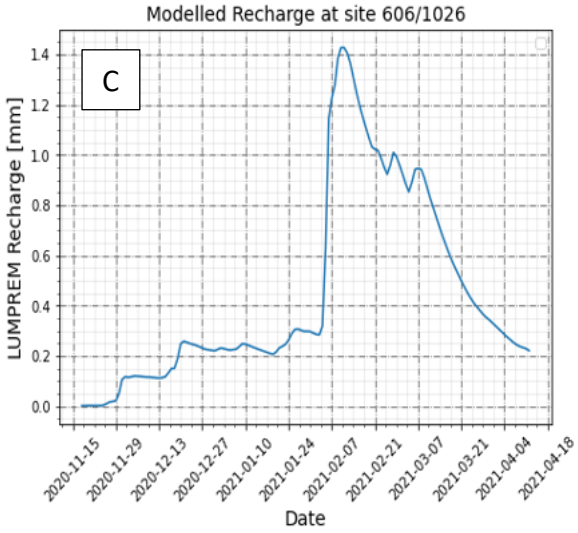

Figure 27: LUMPREM model results and comparison to field measurements at site 606/1026. A) Time series comparison between modelled (black line) and observed piezometric level (red line), including the rainfall input data (dashed purple line) and modelled recharge (blue line). B) Table comparing the attributes of the two time series, showing maximum, minimum and mean values of the modelled and observed data, the sum of the modelled recharge as well as the Pearson and Spearman correlations of the two time series. C) Scaled modelled recharge plot, showing the distribution of the recharge events over the observation period (blue line).

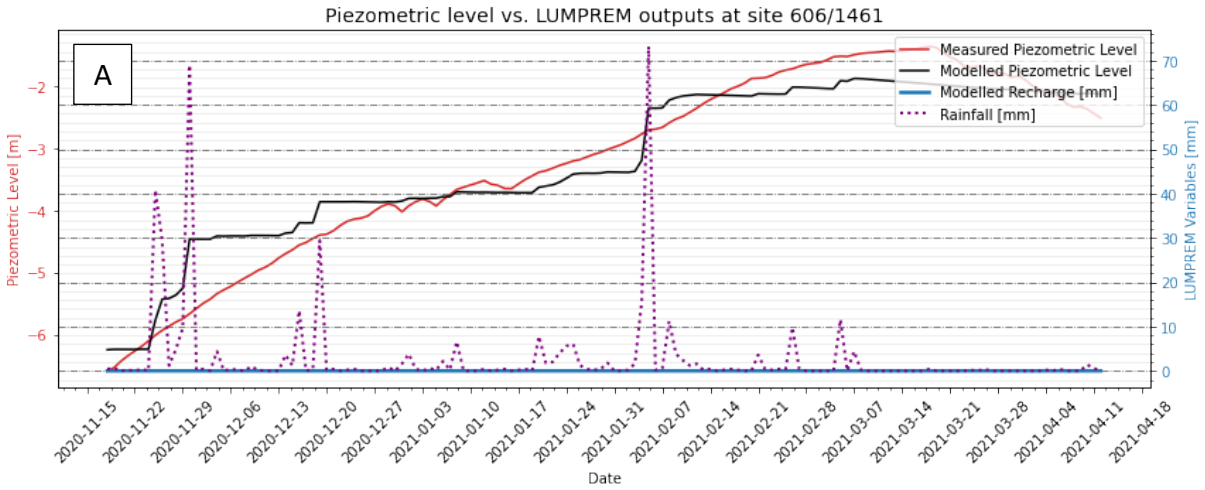

B	Measured Piezometric Level [m]	Modelled Piezometric Level [m]	Recharge [mm]
MAX	-1.36	-1.88	0.01
MIN	-6.59	-6.25	0
MEAN	-3.21	-3.21	0
SUM	-	-	0.37
Pearson-Test	r-value: 0.9746 p-value: 1.8377e-95		
Spearman-Test	r-value: 0.9873 p-value: 5.7802-117		

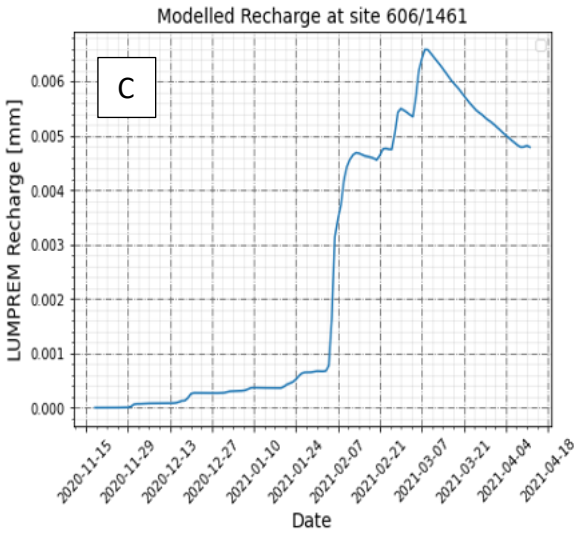

Figure 28: LUMPREM model results and comparison to field measurements at site 606/1461. A) Time series comparison between modelled (black line) and observed piezometric level (red line), including the rainfall input data (dashed purple line) and modelled recharge (blue line). B) Table comparing the attributes of the two time series, showing maximum, minimum and mean values of the modelled and observed data, the sum of the modelled recharge as well as the Pearson and Spearman correlations of the two time series. C) Scaled modelled recharge plot, showing the distribution of the recharge events over the observation period (blue line).

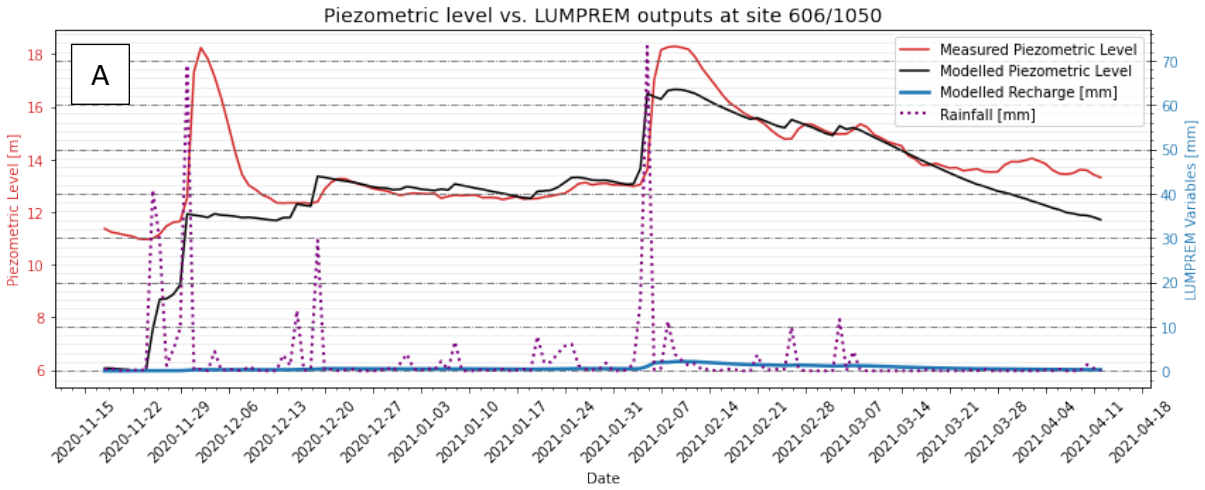

B	Measured Piezometric Level [m]	Modelled Piezometric Level [m]	Recharge [mm]
MAX	18.30	16.66	2.11
MIN	10.96	5.96	0.00
MEAN	13.80	13.00	0.64
SUM	–	–	93.67
Pearson-Test	r-value: 0.7087 p-value: 1.4194e-23		
Spearman-Test	r-value: 0.6690 p-value: 2.7585e-20		

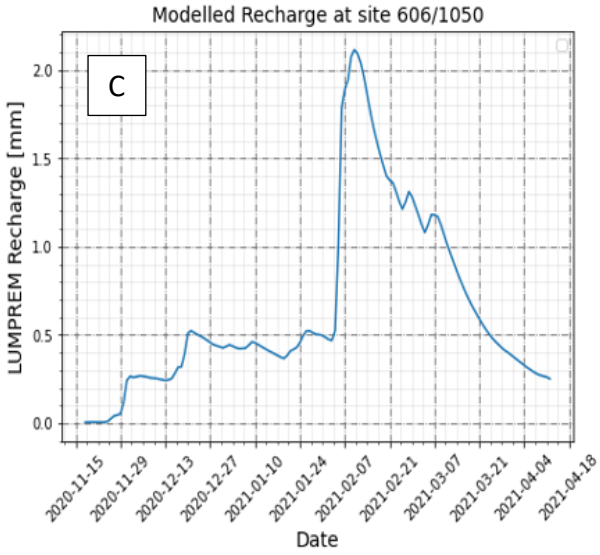

Figure 29: LUMPREM model results and comparison to field measurements at site 606/10. A) Time series comparison between modelled (black line) and observed piezometric level (red line), including the rainfall input data (dashed purple line) and modelled recharge (blue line). B) Table comparing the attributes of the two time series, showing maximum, minimum and mean values of the modelled and observed data, the sum of the modelled recharge as well as the Pearson and Spearman correlations of the two time series. C) Scaled modelled recharge plot, showing the distribution of the recharge events over the observation period (blue line).

5 DISCUSSION

5.1 Temporal and Spatial Distribution of Climate Variables

The strong variability of the climate factors as described in Miranda et al. (2002), seem not to apply within the study area, most likely due to its size, relatively homogeneous topography and proximity to the ocean (Figure 13 & 16). As temperature and precipitation define the evapotranspiration process, all major drivers that induce fluctuations in groundwater are taken under consideration in this study (Figure 20). The amplitude, spatial and temporal distribution of the climate factors were conducted by visualizing and analysing two different data sets, the gridded ERA5 reanalysis data and the records of the DRAP Algarve weather station (DRAP, 2021; ECMWF, 2012). The initial comparison of the two different derived data sets showed high differences, especially regarding the precipitation and its amplitude (Figure 14 & 15). While the ERA5 data projects a total sum of 127.5 mm of rain over the observation period, the weather station recorded the maximum total precipitation of 400.8 mm, which resembles the common idea of the region's rain season (Miranda et al., 2002; Neves et al., 2020a, 2020b; Nunes et al., 2006). The maximum difference between these time series is 66.80 mm, all together leading to the assumption that the weather station provides more accurate representation of reality. Nevertheless, the two data sets show similar trends and present identical temporal distribution between the major rainfall events. Regarding the temperature values of the compared data, the two different derived time series show higher similarities with a maximum difference of only 2.6°C and mostly following identical trends and peaks of the same amplitude.

Under the assumption that the ERA5 data was representative enough for further investigation, the data's gridded variability was used to show spatial distribution differences of the climate variables within the study area. The trilinear interpolation of the four grid points covering the study sites showed very low differences when compared to each other (Figure 13-15). Overall, there are very low to no differences between the four time series derived from the different locations, with a low maximum difference of 1.3 mm in the rain variable and 1.6°C in the temperature variable. The bottom two pixels (A&D) show the lowest variability when compared with each other, but the highest variability compared to the top two pixels (B&C). This indicates that strongest variability, although very low, within the study

area is induced by changes of altitude or distance to the coastline. The contour maps of the two climate variables created over the observation period and the three summer months, support the idea of a low climate variability, indicating very low spatial differences of 0.1 mm of precipitation and temperatures 1.6°C for both time windows (Figure 17). The precipitation values detected during the summer months are negligible, due to their very low amplitude and the fact that the amount of precipitation cannot interfere with the groundwater systems, as the dried out unsaturated zone wouldn't allow deeper percolation. Additionally, the contour maps visualize the latitudinal dependency (South to North) of the climate variables and their spatial distribution (Miranda et al., 2002). However, this local dependency seems to shift over the summer months to a rather East-West trended distribution which may be induced by oscillations or climate waves originating from the Mediterranean Sea (Gonzalez-Hidalgo et al., 2009).

Considering the very low spatial variability within the study area and the higher significance and accuracy of the climate data derived from the weather station, all further computations only included the data derived from the measurements of the DRAP Algarve weather station. A look at the relationship between rainfall, temperature and the evapotranspiration clearly shows the dependency of the evapotranspiration and the climate variables, as the potential evapotranspiration follows along with the trends of the temperature.

5.2 Effect of Climate Variables on Groundwater Levels

The hydrological cycle is rigorously coupled with the fluctuations of atmospheric temperature and radiation correspondences that form climate (Bates et al., 2008). Natural variability that comes with all climate factors directly influences groundwater storages, as it is the main driver of the recharge processes (Kumar, 2012; Thomas & Famiglietti, 2019). Observational data and resulting climate projection indicate a clear evidence of groundwater systems being vulnerable and strongly affected by regional climate along with its seasonality (Green et al., 2011). In this study, the main variables of the climate that drive groundwater fluctuation and their recharge showed to be precipitation and temperature. As seen by the strong positive values of the correlation coefficient, rainfall events have a strong beneficial effect on the groundwater levels (Figure 20).

Whereas the temperature and potential evapotranspiration values negatively affect the groundwater levels, within a weaker scale. Even though temperature and potential evapotranspiration appear to be unrelated, their correlations to the measuring sites are very similar, meaning their effect on the groundwater shows similar amplitudes. Due to evapotranspiration's co-dependency of the available soil moisture, the relationship between evapotranspiration and temperature is weak (Sudheer et al., 2003). Because heat fluxes determine the value of potential evapotranspiration, it will not interact with groundwater at larger scales as the temperature.

The significant rises observed in the piezometric level (Figure 6 – Figure 10) are clearly connected to the strong rainfall events during the observation period. However, the variation of these rises between the sites are most likely to be affected by local abstraction. The general rise of all piezometric measurement is partly controlled by the rebound processes that occur in periods of no pumping, which usually stops in this region in October until March. Depending on the proximity to areas of strong water abstraction and the surrounding hydrogeological conditions, these rebound signals may also vary in intensity and cover some of the observable recharge events within the measurements.

The statistical analysis revealed strong connections between precipitation and piezometric observations across all sites, with all computed correlation coefficients exceeding 0.7. The differences of the correlations between rainfall and groundwater levels of each site can arguably be induced by several factors.

The link between each site and rainfall follows a pattern that reflects the sequence in which each site is distributed from south to north, with the highest correlation found at site 610/179 (the farthest south) and site 606/1050 (the farthest north). While this pattern could indicate inaccuracy caused by the weather station's distance, the low correlation obtained at site 610/180 suggests that there are alternative possibilities creating this trend. Another more plausible explanation for the lowest correlation to rain at sites 610/180 and 606/1050 could be the horizontal arrangement of these two boreholes. Site 610/180 only measure the upper or shallow unconfined aquifer within the Plio-Quaternary. Combined with the effect of pumping, other causes and drivers may overwhelm the rainfall signal as the aquifer is closer to the surface and can easily interact with the atmosphere, resulting in generally reduced correlations.

Given the fact that site 606/1050 appears to correlate relatively poorly with all climate factors compared to the other sites, another factor to consider is the topographic location. A higher topographical location could generate internal flows within the groundwater system, leading to water movement following the downward slope of the lithology towards the south (Almeida et al., 2000; Stigter et al., 2006). This concept could potentially explain the pattern of the piezometric readings at this location. Again, the geological strata this site operates in must be considered. Site 606/1050 uses a relatively deep borehole, which reaches into the Jurassic formations. In the Jurassic, the water movement to the south (following the topography) is likely to be limited by the Cretaceous layer (Figure 3), which almost functions as an aquitard due to its low hydrological conductivity especially in its older layers (bottom layers). This aquitard like behaviour of the lower Cretaceous would explain the higher piezometric variations observed in this system (Figure 5) and could lead to signals in GWL that overwhelm the ones of the climate variable, resulting in low correlations.

After significant rainfalls, the piezometric at site 606/1050 levels generate extreme short living peaks, which then reconfigure into a stable lower rise of the water level. These peaks are results of rapid by-pass recharge induced by fracture network of possible faults or high karstic regions, which is then followed by a slower decline as the water gradually drains. The idea of confined structure of M10 aquifer, where site 606/1050 is located in, can additionally be justified when comparing the relationships between the measurements of each site (Figure 21), as this site has relatively low correlates compared to the others (coefficients around 0.5), while all sites located in the M12 are highly correlated with each other (coefficients above 0.9).

The computed cross-correlation reveals no significant lags between the data sets, implying that the groundwater at all study sites responds to climate factors immediately. Because the cross-correlation only calculates the signal’s first appearance within a time series, it's important to note that the recharging events, when seen as rises in the piezometric level, have various gradients depending on the measurement location. While sites 610/179, 610/180 and 606/1050 show very sharp rises when major rainfall events occur, sites 606/1026 and 606/1461 indicate gradual rise. The geology and hydrological conductivity of the area dictate the gradients of recharge events (Healy et al., 2007; Morris & Johnson, 1967).

A sharp short recharge indicates a rather porous media, higher karstic surrounding or a nearby fault system, which enables fast movement of water through the ground. A gradual recharge suggests a lack of all these geological attributes and formations or a considerable distance to geological formations, all of which allow for rapid recharging of a groundwater system (Corona et al., 2018; Jourde et al., 2015).

5.3 The BALSEQ Model

The BALSEQ model (Ferreira, 1981) was run with the climate collected within this study and calibrated based on previous approaches of its use at the study area (Ferreira & Rodrigues, 1988; Martins et al., 2021). The model's simplicity makes it suitable for use in areas with limited access to information and data, such as the Algarve. However, the calibration values CN and AGUT allow large variances in the outputs. These two variables are mainly determined by the conceptual appearance of the geological surrounding, which may highly vary depending on the scales, maps, factors and norms considered by the user, as seen in the two referred approaches. It is imperative to note that the conceptual model BALSEQ follows disregards any negative influences on the groundwater, such as climate driven negative fluxes or internal flows that dispense water, leading to only positive trended recharge outputs. The very direct and linear approach of this model also ignores the travel times of processes as percolation and infiltration, hence the better correlated results when the Savitzky-Golay filter was applied to the cumulative recharge. The model's linear nature also makes it difficult to compare the model's outputs to observable measurements, as the only way to connect the model to reality is to run a correlation test between the cumulative recharge and the recorded piezometric level. Multiple iterations of the model with variations of the CN and AGUT values showed that the correlation coefficient consistently increases with the increase of each variable.

The findings of the two BALSEQ calibrations presented reveal significant discrepancies (Figure 23). Model A simulates a total recharge of 160.83 mm over the observation period, replicating the findings of Ferreira & Rodrigues (1988). Model B simulates with a total recharge of 81.85 mm generally higher correlations to the field observations, demonstrating the potential differences between the iterations.

Regarding the correlations between the piezometric measurements and the cumulative recharge output of the model (with Savitzky-Golay filter), sites 610/179, 606/1026 and 606/1461 all scored very high, with all coefficients being above 0.8. Whereas sites 610/180 and 606/1050 showed relatively low correlations. Comparing the measurements with the simulated soil moisture storage, revealed that only site 610/180 and site 606/1050 have positive correlations to this output variable. This again emphasizes the linearity problem of this model, having no negative fluxes within the recharge simulation.

Because site 610/180 is thought to be in the upper aquifers where stronger variations are created due to higher connectivity to the atmosphere (de Vries & Simmers, 2002), their simulation in this model would be better depicted in the soil moisture variable rather than the actual recharge.

5.4 The LUMPREM Model

The groundwater head simulation in the LUMPREM model allows an extremely site-specific calibration. Five unique models with manually calibrated input variables were created to obtain the maximum correlations between observed and simulated piezometric data for each site. The LUMPREM model's complexity and number of interchangeable input variables allow a simulation that considers detailed percolation and infiltration processes as well as interactions with the atmosphere (Doherty, 2020). However, the quantity of these parameters may have a negative impact on the outcomes due to additional uncertainty (Aguilera & Murillo, 2009; Moeck et al., 2020). The model simulates recharge as a continuously discharging bucket model, whose transport efficiency varies with soil moisture content, using the climate variables collected within this study as input. When simulating lower semi-confined aquifers, such as site 610/179, 606/1026, and 606/1461, this concept is demonstrated (Figure 26,27 & 28). Only the last rainfall events at the end of the observation period cause the relatively low computed total recharge at these sites. This suggests that the deeper aquifer only receives replenishing water after all the layers and systems above have been saturated to some extent. In comparison, the simulation within the upper aquifer at sites 610/180 and 606/1050 indicate larger responses of the recharge value to rainfall events at the start of the observation period (Figure 25 & 29).

Although all correlations between each observation and its simulation are very high, the computed total amount of recharge seems to be too low, when compared to the results given by the BALSEQ model. These very low values of recharge, especially at site 606/1461, are most likely results of the very site-specific calibration. The model's well-defined geophysical definitions for reproducing piezometric levels may result in the assumption of extreme and unrealistic geological formations with exceedingly poor hydrological conductivity that prevents recharge. These assumptions could be the result of misunderstandings due to this site-specific approach, where other aspects like topography and fault systems were ignored, which may explain an observed groundwater level without artificially reducing the computed recharge or internal flow.

5.5 Comparison of the Applied Models

The existence and sustainability of groundwater resources are governed by groundwater recharge events (Moeck et al., 2020). Estimating recharge quantities allows for the evaluation of the system's renewability as well as its vulnerability through climate extremes such as droughts (Walker et al., 2019). Depending on the environment in which it is intended to operate, each technique or method has limitations in terms of application and reliability (Xu & Beekman, 2019). Therefore, a complete understanding of the studied area's hydroclimatic characteristics and geological setting is required (Aguilera & Murillo, 2009). Outputs of groundwater recharge estimates often range amongst methods due to the uncertainties inherent in each method, their varying spatiotemporal scales at which they operate and their form of recharge they reflect. Consequently, it is common practice to implement a variety of techniques. Inaccuracies caused to one model’s assumption may only become noticeable when comparing results amongst different methods (Walker et al., 2019). Recognizing these discrepancies in multi-method comparison may however provide valuable insights into the hydrogeological system by integrating all the information and characteristics they propose (Moeck et al., 2020; Walker et al., 2019).

Several approaches and methodologies were examined and combined in this study, resulting in primarily two models with good performance.

Although the LUMPREM and BALSEQ models have a similar conceptual structure when comparing their outcomes, the contrasts in complexity become evident. While the BALSEQ model predicts recharge quantities between 81.58 mm and 160.32 mm (Fgure 23), depending on its calibration, the LUMPREM model ranges between 16.97 and 93.67 mm of a simulation total recharge (Figure 25-29).

The relatively high quantities of recharge simulated by the BALSEQ model are most likely due to its simplicity. While this model ignores hydrogeological processes that would most likely decrease the amount of recharge (Lohman, 1972), it also ignores systems or geological formations such as faults or karstic formations that enable higher quantities of recharge (Allocca et al., 2015). Within an approach of estimating recharge over a larger and geologically heterogeneous area as in this case (Stigter et al., 1998, 2006), the neglection of both, positive and negative influencing recharge factors, might compensate within the area and lead to realistic computations.

The rather low recharge simulated within the LUMPREM model might be the result of not compensating recharge inducing and reducing factors over a region. The LUMPREM model, as used in this study, computes recharge by assuming geological columns that may reproduce the observed groundwater behaviour. While this includes hydrogeological processes that are expected to have a negative impact on recharge, LUMPREM is limited in representing elements that may cause greater recharge values (karstic development, faults, topography), resulting in adversely biased findings. Nonetheless, LUMPREM provides a better understanding of the processes occurring within the groundwater system and may even contribute to the detection and definition of the subsurface.

After all, both the BALSEQ and the LUMPREM models provide total recharge findings that coincide in the 80-90 mm range. As a result, both models may complement each other and contribute to the detection of bias tendencies. The models' usage and comparison allow for the justification of calibration ranges as well as the gathering of more detailed information about the entire system and its processes.

6 CONCLUSION

Estimation of recharge is one of the most complicated parts of hydrogeology, and yet, one of the most crucial, as difficult water resource management decisions are based on the concept of sustainable yield, a proportion of annual recharge at which water levels are stable.

This study provides a detailed investigation of a small water-shed aquifer system in the semi-arid environment of the Algarve, as well as its interaction and behaviour with and due to its climatic and hydrogeological surroundings, in order to develop and run recharge estimation algorithms. Two recharge models were effectively calibrated to the local condition and input data, producing simulations that differed significantly. Although the two models complement each other and lead to realistic results, it is imperative to acknowledge the remaining uncertainties. These uncertainties are mostly caused by the conceptual models on which each simulation is based, as well as the study area's extremely diverse geology. This study shows the extreme variations between different simulation approaches and emphasizes the lack of confidence one may have in these estimates as well as the careful use of their results for water management.

A comparable strategy, as given in this work, might collect highly thorough information on the research area, resulting in a solid knowledge of the study area’s regional hydrogeology, by incorporating more and effectively dispersed sample sites, while using more estimation methods of different origin. Because groundwater resources, particularly in the Algarve, are known to be threatened by climatic extremes, it is necessary to investigate and comprehend all aspects of these groundwater systems. This study offers a feasible starting point for such an inquiry.

References

Aguilera, H., & Murillo, J. M. (2009). The effect of possible climate change on natural groundwater recharge based on a simple model: A study of four karstic aquifers in SE Spain. *Environmental Geology*, *57*(5), 963–974. https://doi.org/10.1007/s00254-008-1381-2

Aishlin, P., & Mcnamara, J. P. (2011). Bedrock infiltration and mountain block recharge accounting using chloride mass balance. *Hydrological Processes*, *25*(12). https://doi.org/10.1002/hyp.7950

Allocca, V., de Vita, P., Manna, F., & Nimmo, J. R. (2015). Groundwater recharge assessment at local and episodic scale in a soil mantled perched karst aquifer in southern Italy. *Journal of Hydrology*, *529*(P3), 843–853. https://doi.org/10.1016/j.jhydrol.2015.08.032

Almeida, C., Mendoça, J. J. L., Jesus, M. R., & Gomes, A. J. (2000). SistemasAquiferosdePortugalContinental-VolumeI. *Relatório INAG, Instituto Da Água, Lisbon*.

APA. (2021). *Agência Portuguesa do Ambiente (Portugues Environment Agency)*. https://rea.apambiente.pt/

Arnold, J. G., & Allen, P. M. (1999). Automated methods for estimating baseflow and ground water recharge from streamflow records. *Journal of the American Water Resources Association*, *35*(2). https://doi.org/10.1111/j.1752-1688.1999.tb03599.x

Arora, B., Dwivedi, D., Faybishenko, B., Jana, R. B., & Wainwright, H. M. (2019). Understanding and Predicting Vadose Zone Processes. *Reviews in Mineralogy and Geochemistry*, *85*(1), 303–328. https://doi.org/10.2138/rmg.2019.85.10

Bates, B. C. (Bryson C.), Kundzewicz, Z., Wu, S., Palutikof, J., & Intergovernmental Panel on Climate Change. Working Group II. (2008). *Climate change and water*.

Belo-Pereira, M., Dutra, E., & Viterbo, P. (2011). Evaluation of global precipitation data sets over the Iberian Peninsula. *Journal of Geophysical Research Atmospheres*, *116*(20). https://doi.org/10.1029/2010JD015481

Besser, H., Mokadem, N., Redhouania, B., Rhimi, N., Khlifi, F., Ayadi, Y., Omar, Z., Bouajila, A., & Hamed, Y. (2017). GIS-based evaluation of groundwater quality and estimation of soil

salinization and land degradation risks in an arid Mediterranean site (SW Tunisia). *Arabian Journal of Geosciences*, *10*(16). https://doi.org/10.1007/s12517-017-3148-0

Breuer, L., Huisman, J. A., Willems, P., Bormann, H., Bronstert, A., Croke, B. F. W., Frede, H. G., Gräff, T., Hubrechts, L., Jakeman, A. J., Kite, G., Lanini, J., Leavesley, G., Lettenmaier, D. P., Lindström, G., Seibert, J., Sivapalan, M., & Viney, N. R. (2009). Assessing the impact of land use change on hydrology by ensemble modeling (LUCHEM). I: Model intercomparison with current land use. *Advances in Water Resources*, *32*(2). https://doi.org/10.1016/j.advwatres.2008.10.003

Cambraia Neto, A. J., & Rodrigues, L. N. (2020). Evaluation of groundwater recharge estimation methods in a watershed in the Brazilian Savannah. *Environmental Earth Sciences*, *79*(6). https://doi.org/10.1007/s12665-020-8884-x

Cardoso, R. M., Soares, P. M. M., Lima, D. C. A., & Miranda, P. M. A. (2019). Mean and extreme temperatures in a warming climate: EURO CORDEX and WRF regional climate high-resolution projections for Portugal. *Climate Dynamics*, *52*(1–2). https://doi.org/10.1007/s00382-018-4124-4

Chen, J., Jönsson, P., Tamura, M., Gu, Z., Matsushita, B., & Eklundh, L. (2004). A simple method for reconstructing a high-quality NDVI time-series data set based on the Savitzky-Golay filter. *Remote Sensing of Environment*, *91*(3–4). https://doi.org/10.1016/j.rse.2004.03.014

Choudri, B. S. (2004). *Estimation of Surface Run-off and Groundwater Recharge Using Daily Sequential Water Balance Model the "BALSEQ": Application in Goa Mining Area Planning of Sustainable Regeneration of Mining Areas using Tri-Sector Partnership View project Assessment of Sustainable Remediation Options for Contaminated Soil Stockpiles (Phase 1: Characterization of the Contamination Level) View project*. https://www.researchgate.net/publication/258073724

Corona, C. R., Gurdak, J. J., Dickinson, J. E., Ferré, T. P. A., & Maurer, E. P. (2018). Climate variability and vadose zone controls on damping of transient recharge. *Journal of Hydrology*, *561*, 1094–1104. https://doi.org/10.1016/j.jhydrol.2017.08.028

Crosbie, R. S., McCallum, J. L., Walker, G. R., & Chiew, F. H. S. (2012). Episodic recharge and climate change in the Murray-Darling Basin, Australia. *Hydrogeology Journal*, *20*(2). https://doi.org/10.1007/s10040-011-0804-4

Cuthbert, M. O., Taylor, R. G., Favreau, G., Todd, M. C., Shamsudduha, M., Villholth, K. G., MacDonald, A. M., Scanlon, B. R., Kotchoni, D. O. V., Vouillamoz, J. M., Lawson, F. M. A., Adjomayi, P. A., Kashaigili, J., Seddon, D., Sorensen, J. P. R., Ebrahim, G. Y., Owor, M., Nyenje, P. M., Nazoumou, Y., … Kukuric, N. (2019). Observed controls on resilience of groundwater to climate variability in sub-Saharan Africa. *Nature*, *572*(7768), 230–234. https://doi.org/10.1038/s41586-019-1441-7

de Castro, J., Ballesteros, F., Méndez, A., & Tarquis, A. M. (2014). Fractal analysis of laplacian pyramidal filters applied to segmentation of soil images. *Scientific World Journal*, *2014*. https://doi.org/10.1155/2014/212897

de Vries, J. J., & Simmers, I. (2002). Groundwater recharge: An overview of process and challenges. *Hydrogeology Journal*, *10*(1), 5–17. https://doi.org/10.1007/s10040-001-0171-7

Dickinson, J. E., Hanson, R. T., & Predmore, S. K. (2014). HydroClimATe: hydrologic and climatic analysis toolkit. In *Techniques and Methods*. https://doi.org/10.3133/tm4a9

Doherty, J. (2020). *A Simple Lumped Parameter Model for Unsaturated Zone Processes*. https://pesthomepage.org/programs

DRAP. (2021). *Direcção Regional De Agricultura E Pescas Do Algarve - DRAP*. http://www.drapalgarve.gov.pt/ema/pat.htm

ECMWF. (2012). *ERA5-Land hourly data from 1981 to present, European Centre for Medium-Range Weather Forecasts*. https://doi.org/https://doi.org/10.24381/cds.e2161bac

European Commission. (2015). *Management Plans Member State: PORTUGA: "The Water Framework Directive and the Floods Directive: Actions towards the "good status" of EU water and to reduce flood risks "*. https://ec.europa.eu/environment/water/water-framework/pdf/4th_report/MS%20annex-Portugal.pdf

Famiglietti, J. S. (2014). The global groundwater crisis. In *Nature Climate Change* (Vol. 4, Issue 11, pp. 945–948). Nature Publishing Group. https://doi.org/10.1038/nclimate2425

Ferreira, J. P. L. (1981). *Mathematical model for the evaluation of the recharge of aquifers in semiarid regions with lack of hydrogeological data.*

Ferreira, J. P. L., & Rodrigues, J. D. (1988). BALSEQ — A Model for the Estimation of Water Balances, Including Aquifer Recharges, Requiring Scarce Hydrologic Data. In *Estimation of Natural Groundwater Recharge*. https://doi.org/10.1007/978-94-015-7780-9_19

Francés, A. P., Ramalho, E. C., Fernandes, J., Groen, M., de Plaen, J., Hugman, R., Khalil, M. A., & Santos, F. A. M. (2014). Hydrogeophysics contribution to the development of hydrogeological conceptual model of coastal aquifers – Albufeira-Ribeira de Quarteira aquifer case study. *Assemblia Luso Espanhola de Geodesia e Geofisica*, *Evora 2014*.

Francés, A. P., Ramalho, E. C., Fernandes, J., Groen, M., Hugman, R., Khalil, M. A., de Plaen, J., & Monteiro Santos, F. A. (2015). Contributions of hydrogeophysics to the hydrogeological conceptual model of the Albufeira-Ribeira de Quarteira coastal aquifer in Algarve, Portugal. *Hydrogeology Journal*, *23*(7). https://doi.org/10.1007/s10040-015-1282-x

Gonzalez-Hidalgo, J. C., Lopez-Bustins, J. A., Štepánek, P., Martin-Vide, J., & de Luis, M. (2009). Monthly precipitation trends on the Mediterranean fringe of the Iberian Peninsula during the second-half of the twentieth century (1951-2000). *International Journal of Climatology*, *29*(10). https://doi.org/10.1002/joc.1780

Gouveia, C. M., Bastos, A., Trigo, R. M., & Dacamara, C. C. (2012). Drought impacts on vegetation in the pre- and post-fire events over Iberian Peninsula. *Natural Hazards and Earth System Science*, *12*(10). https://doi.org/10.5194/nhess-12-3123-2012

Green, T. R., Taniguchi, M., Kooi, H., Gurdak, J. J., Allen, D. M., Hiscock, K. M., Treidel, H., & Aureli, A. (2011). Beneath the surface of global change: Impacts of climate change on groundwater. In *Journal of Hydrology* (Vol. 405, Issues 3–4, pp. 532–560). https://doi.org/10.1016/j.jhydrol.2011.05.002

Healy, R. W., Winter, T. C., LaBaugh, J. W., & Franke, O. L. (2007). *Water Budgets: Foundations for Effective Water-Resources and Environmental Management*. https://pubs.usgs.gov/circ/2007/1308/index.html

Helldén, U., & Tottrup, C. (2008). Regional desertification: A global synthesis. *Global and Planetary Change*, *64*(3–4). https://doi.org/10.1016/j.gloplacha.2008.10.006

Howell, T. A., & Evett, S. R. (2001). The Penman-Monteith Method. *Bushland, Texas: USDA Agricultural Research Service*.

Hugman, R., Stigter, T., Costa, L., & Monteiro, J. P. (2017). Modeling Nitrate-contaminated Groundwater Discharge to the Ria Formosa Coastal Lagoon (Algarve, Portugal). *Procedia Earth and Planetary Science*, *17*. https://doi.org/10.1016/j.proeps.2016.12.174

Hugman, R., Stigter, T. Y., Monteiro, J. P., & Nunes, L. (2012). Influence of aquifer properties and the spatial and temporal distribution of recharge and abstraction on sustainable yields in semi-arid regions. *Hydrological Processes*, *26*(18). https://doi.org/10.1002/hyp.8353

IPMA. (2021). *IPMA-Instituto Português do Mar a e da Atmosfera (Portuguese Institute of Sea Atmosphere)*. https://www.ipma.pt/

Jolly, W. M., Cochrane, M. A., Freeborn, P. H., Holden, Z. A., Brown, T. J., Williamson, G. J., & Bowman, D. M. J. S. (2015). Climate-induced variations in global wildfire danger from 1979 to 2013. *Nature Communications*, *6*. https://doi.org/10.1038/ncomms8537

Jourde, H., Mazzilli, N., Lecoq, N., Arfib, B., & Bertin, D. (2015). KARSTMOD: A generic modular reservoir model dedicated to spring discharge modeling and hydrodynamic analysis in karst. *Environmental Earth Sciences*, *1*, 339–344. https://doi.org/10.1007/978-3-642-17435-3_38

Kottek, M., Grieser, J., Beck, C., Rudolf, B., & Rubel, F. (2006). World map of the Köppen-Geiger climate classification updated. *Meteorologische Zeitschrift*, *15*(3). https://doi.org/10.1127/0941-2948/2006/0130

Kumar, C. P. (2012). Climate Change and Its Impact on Groundwater Resources. *RESEARCH INVENTY: International Journal of Engineering and Science*, *1*(5).

le Houérou, H. N. (1996). Climate change, drought and desertification. In *Journal of Arid Environments* (Vol. 34, Issue 2). https://doi.org/10.1006/jare.1996.0099

Lewis, M. F., & Walker, G. R. (2002). Assessing the potential for significant and episodic recharge in southern Australia using rainfall data. *Hydrogeology Journal*, *10*(1). https://doi.org/10.1007/s10040-001-0172-6

Liang, X., & Zhang, Y. K. (2012). A new analytical method for groundwater recharge and discharge estimation. *Journal of Hydrology*, *450–451*. https://doi.org/10.1016/j.jhydrol.2012.05.036

Lima, T. A. S. (2020). *Caracterização hidrogeológica e uso da água de um sector das areias, arenitos e cascalheiras do litoral do Baixo Alentejo*.

Lohman, S. W. (1972). *Ground-Water Hydraulics*. https://pubs.er.usgs.gov/publication/pp708

Maréchal, J. C., Dewandel, B., Ahmed, S., Galeazzi, L., & Zaidi, F. K. (2006). Combined estimation of specific yield and natural recharge in a semi-arid groundwater basin with

irrigated agriculture. *Journal of Hydrology*, *329*(1–2). https://doi.org/10.1016/j.jhydrol.2006.02.022

Martins, T. N., Mendes Oliveira, M., Portela, M. M., & Eira Leitão, T. (2021). Sensitivity analysis of a simplified precipitation-runoff model to estimate water availability in Southern Portuguese watersheds. *Acque Sotterranee - Italian Journal of Groundwater*, *10*(2), 33–47. https://doi.org/10.7343/as-2021-514

Marvel, K., Cook, B. I., Bonfils, C. J. W., Durack, P. J., Smerdon, J. E., & Williams, A. P. (2019). Twentieth-century hydroclimate changes consistent with human influence. *Nature*, *569*(7754), 59–65. https://doi.org/10.1038/s41586-019-1149-8

Mazzilli, N., Guinot, V., Jourde, H., Lecoq, N., Labat, D., Arfib, B., Baudement, C., Danquigny, C., Dal Soglio, L., & Bertin, D. (2019). KarstMod: A modelling platform for rainfall - discharge analysis and modelling dedicated to karst systems. *Environmental Modelling and Software*, *122*. https://doi.org/10.1016/j.envsoft.2017.03.015

Meixner, T., Manning, A. H., Stonestrom, D. A., Allen, D. M., Ajami, H., Blasch, K. W., Brookfield, A. E., Castro, C. L., Clark, J. F., Gochis, D. J., Flint, A. L., Neff, K. L., Niraula, R., Rodell, M., Scanlon, B. R., Singha, K., & Walvoord, M. A. (2016). Implications of projected climate change for groundwater recharge in the western United States. In *Journal of Hydrology* (Vol. 534, pp. 124–138). Elsevier B.V. https://doi.org/10.1016/j.jhydrol.2015.12.027

Miranda, P. M., Rodrigues Tomé, A., & Valente, M. A. (2002). *20th Century Portuguese Climate and Climate Scenarios in Climate Change in Portugal: Scenarios, Impacts and Adaptation*. https://www.researchgate.net/publication/257427857_20th_Century_Portuguese_Climate_and_Climate_Scenarios_in_Climate_Change_in_Portugal_Scenarios_Impacts_and_Adaptation

Moeck, C., Grech-Cumbo, N., Podgorski, J., Bretzler, A., Gurdak, J. J., Berg, M., & Schirmer, M. (2020). A global-scale dataset of direct natural groundwater recharge rates: A review of variables, processes and relationships. *Science of the Total Environment*, *717*. https://doi.org/10.1016/j.scitotenv.2020.137042

Moeck, C., von Freyberg, J., & Schirmer, M. (2018). Groundwater recharge predictions in contrasted climate: The effect of model complexity and calibration period on recharge

rates. *Environmental Modelling and Software*, *103*, 74–89. https://doi.org/10.1016/j.envsoft.2018.02.005

Moon, S. K., Woo, N. C., & Lee, K. S. (2004). Statistical analysis of hydrographs and water-table fluctuation to estimate groundwater recharge. *Journal of Hydrology*, *292*(1–4). https://doi.org/10.1016/j.jhydrol.2003.12.030

Morris, D. A., & Johnson, A. I. (1967). *Summary of hydrologic and physical properties of rock and soil materials, as analyzed by the hydrologic laboratory of the U.S. Geological Survey, 1948-60*. https://doi.org/10.3133/wsp1839D

Mualem, Y. (1976). A new model for predicting the hydraulic conductivity of unsaturated porous media. *Water Resources Research* , *12*, 513–522.

Neves, M. C., Costa, L., Hugman, R., & Monteiro, J. P. (2019). The impact of atmospheric teleconnections on the coastal aquifers of Ria Formosa (Algarve, Portugal). *Hydrogeology Journal*, *27*(8), 2775–2787. https://doi.org/10.1007/s10040-019-02052-6

Neves, M. C., Nunes, L. M., & Monteiro, J. P. (2020a). Evaluation of GRACE data for water resource management in Iberia: a case study of groundwater storage monitoring in the Algarve region. *Journal of Hydrology: Regional Studies*, *32*. https://doi.org/10.1016/j.ejrh.2020.100734

Neves, M. C., Nunes, L. M., & Monteiro, J. P. (2020b). Evaluation of GRACE data for water resource management in Iberia: a case study of groundwater storage monitoring in the Algarve region. *Journal of Hydrology: Regional Studies*, *32*. https://doi.org/10.1016/j.ejrh.2020.100734

Nimmo, J. R., & Perkins, K. S. (2018). Episodic Master Recession Evaluation of Groundwater and Streamflow Hydrographs for Water-Resource Estimation. *Vadose Zone Journal*, *17*(1), 180050. https://doi.org/10.2136/vzj2018.03.0050

Nunes, L., Monteiro, J. P., Cunha, M. C., Vieira, J., Lucas, H., & Ribeiro, L. (2006). The water crisis in southern Portugal: How did we get there and how should we solve it. *WIT Transactions on Ecology and the Environment*, *99*, 435–444. https://doi.org/10.2495/RAV060431

Orlanski, I. (1975). A rational subdivision of scales for atmospheric processes. *Bulletin of the American Meteorological Society*, *56*(5).

Rouhani, H., & Malekian, A. (2013). *Automated Methods for Estimating Baseflow from Streamflow Records in a Semi Arid Watershed*. http://jdesert.ut.ac.ir

Salvador, N., Monteiro, J. P., Hugman, R., Stigter, T. Y., & Reis, E. (2012). Quantifying and modelling the contribution of streams that recharge the Querença-Silves aquifer in the south of Portugal. *Natural Hazards and Earth System Sciences*, *12*(11). https://doi.org/10.5194/nhess-12-3217-2012

Scibek, J., & Allen, D. M. (2006). Comparing modelled responses of two high-permeability, unconfined aquifers to predicted climate change. *Global and Planetary Change*, *50*(1–2). https://doi.org/10.1016/j.gloplacha.2005.10.002

Siebert, S., Burke, J., Faures, J. M., Frenken, K., Hoogeveen, J., Döll, P., & Portmann, F. T. (2010). Groundwater use for irrigation - A global inventory. *Hydrology and Earth System Sciences*, *14*(10), 1863–1880. https://doi.org/10.5194/hess-14-1863-2010

Sitch, S., Smith, B., Prentice, I. C., Arneth, A., Bondeau, A., Cramer, W., Kaplan, J. O., Levis, S., Lucht, W., Sykes, M. T., Thonicke, K., & Venevsky, S. (2003). Evaluation of ecosystem dynamics, plant geography and terrestrial carbon cycling in the LPJ dynamic global vegetation model. *Global Change Biology*, *9*(2). https://doi.org/10.1046/j.1365-2486.2003.00569.x

SNIRH. (2021). *Sistema Nacional de Informação de Recursos Hídricos - Portuguese National System for Water Resources Information*. https://snirh.apambiente.pt/

Soares, P. M. M., Cardoso, R. M., Lima, D. C. A., & Miranda, P. M. A. (2017). Future precipitation in Portugal: high-resolution projections using WRF model and EURO-CORDEX multi-model ensembles. *Climate Dynamics*, *49*(7–8). https://doi.org/10.1007/s00382-016-3455-2

Soil Survey Staff. (2014). Kellogg Soil Survey Laboratory Methods Manual. Soil Survey Investigations Report No. 42, Version 5.0. In *Kellogg Soil Survey Laboratory Methods Manual* (Issue 42).

Spinoni, J., Vogt, J. V., Naumann, G., Barbosa, P., & Dosio, A. (2018). Will drought events become more frequent and severe in Europe? *International Journal of Climatology*. https://doi.org/10.1002/joc.5291

Stigter, T. Y., Ribeiro, L., & Dill, A. M. M. C. (2006). Evaluation of an intrinsic and a specific vulnerability assessment method in comparison with groundwater salinisation and

nitrate contamination levels in two agricultural regions in the south of Portugal. *Hydrogeology Journal*, *14*(1–2), 79–99. https://doi.org/10.1007/s10040-004-0396-3

Stigter, T. Y., van Ooijen, S. P. J., Post, V. E. A., Appelo, C. A. J., & Carvalho Dill, A. M. M. (1998). A hydrogeological and hydrochemical explanation of the groundwater composition under irrigated land in a Mediterranean environment, Algarve, Portugal. *Journal of Hydrology* , *208*, 262–279.

Sudheer, K. P., Gosain, A. K., & Ramasastri, K. S. (2003). Estimating Actual Evapotranspiration from Limited Climatic Data Using Neural Computing Technique. *Journal of Irrigation and Drainage Engineering*, *129*(3). https://doi.org/10.1061/(asce)0733-9437(2003)129:3(214)

Tapley, B. D., Bettadpur, S., Ries, J. C., Thompson, P. F., & Watkins, M. M. (2004). GRACE measurements of mass variability in the Earth system. *Science*, *305*(5683). https://doi.org/10.1126/science.1099192

Taylor, R. G., Scanlon, B., Döll, P., Rodell, M., van Beek, R., Wada, Y., Longuevergne, L., Leblanc, M., Famiglietti, J. S., Edmunds, M., Konikow, L., Green, T. R., Chen, J., Taniguchi, M., Bierkens, M. F. P., Macdonald, A., Fan, Y., Maxwell, R. M., Yechieli, Y., … Treidel, H. (2013). Ground water and climate change. In *Nature Climate Change* (Vol. 3, Issue 4, pp. 322–329). https://doi.org/10.1038/nclimate1744

Thomas, B. F., & Famiglietti, J. S. (2019). Identifying Climate-Induced Groundwater Depletion in GRACE Observations. *Scientific Reports*, *9*(1). https://doi.org/10.1038/s41598-019-40155-y

Turnadge, C., & Smerdon, B. D. (2014). A review of methods for modelling environmental tracers in groundwater: Advantages of tracer concentration simulation. In *Journal of Hydrology* (Vol. 519, Issue PD). https://doi.org/10.1016/j.jhydrol.2014.10.056

van Essen. (2021). *Van Essen Intrsuments*. https://www.vanessen.com/

van Genuchten, M. Th. (1980). A Closed-form Equation for Predicting the Hydraulic Conductivity of Unsaturated Soils. *Soil Science Society of America Journal*, *44*(5). https://doi.org/10.2136/sssaj1980.03615995004400050002x

Wada, Y., van Beek, L. P. H., van Kempen, C. M., Reckman, J. W. T. M., Vasak, S., & Bierkens, M. F. P. (2010). Global depletion of groundwater resources. *Geophysical Research Letters*, *37*(20). https://doi.org/10.1029/2010GL044571

Walker, D., Parkin, G., Schmitter, P., Gowing, J., Tilahun, S. A., Haile, A. T., & Yimam, A. Y. (2019). Insights From a Multi-Method Recharge Estimation Comparison Study. *Groundwater*, *57*(2), 245–258. https://doi.org/10.1111/gwat.12801

Weber, K., & Stewart, M. (2004). A critical analysis of the cumulative rainfall departure concept. *Ground Water*, *42*(6). https://doi.org/10.1111/j.1745-6584.2004.t01-11-.x

Wu, W. Y., Lo, M. H., Wada, Y., Famiglietti, J. S., Reager, J. T., Yeh, P. J. F., Ducharne, A., & Yang, Z. L. (2020). Divergent effects of climate change on future groundwater availability in key mid-latitude aquifers. *Nature Communications*, *11*(1). https://doi.org/10.1038/s41467-020-17581-y

Xu, Y., & Beekman, H. E. (2019). Review: Groundwater recharge estimation in arid and semi-arid southern Africa. In *Hydrogeology Journal* (Vol. 27, Issue 3). https://doi.org/10.1007/s10040-018-1898-8

Xu, Y., & van Tonder, G. J. (2001). Estimation of recharge using a revised CRD method. *Water SA*, *27*(3). https://doi.org/10.4314/wsa.v27i3.4977